

RESEARCH ARTICLE

Drosophila Insulin receptor regulates the persistence of injury-induced nociceptive sensitization

Seol Hee Im^{1,*‡}, Atit A. Patel², Daniel N. Cox² and Michael J. Galko^{1,3,‡}

ABSTRACT

Diabetes-associated nociceptive hypersensitivity affects diabetic patients with hard-to-treat chronic pain. Because multiple tissues are affected by systemic alterations in insulin signaling, the functional locus of insulin signaling in diabetes-associated hypersensitivity remains obscure. Here, we used *Drosophila* nociception/nociceptive sensitization assays to investigate the role of Insulin receptor (Insulin-like receptor, InR) in nociceptive hypersensitivity. *InR* mutant larvae exhibited mostly normal baseline thermal nociception (absence of injury) and normal acute thermal hypersensitivity following UV-induced injury. However, their acute thermal hypersensitivity persists and fails to return to baseline, unlike in controls. Remarkably, injury-induced persistent hypersensitivity is also observed in larvae that exhibit either type 1 or type 2 diabetes. Cell type-specific genetic analysis indicates that *InR* function is required in multidendritic sensory neurons including nociceptive class IV neurons. In these same nociceptive sensory neurons, only modest changes in dendritic morphology were observed in the *InR^{RNAi}*-expressing and diabetic larvae. At the cellular level, *InR*-deficient nociceptive sensory neurons show elevated calcium responses after injury. Sensory neuron-specific expression of *InR* rescues the persistent thermal hypersensitivity of *InR* mutants and constitutive activation of *InR* in sensory neurons ameliorates the hypersensitivity observed with a type 2-like diabetic state. Our results suggest that a sensory neuron-specific function of *InR* regulates the persistence of injury-associated hypersensitivity. It is likely that this new system will be an informative genetically tractable model of diabetes-associated hypersensitivity.

KEY WORDS: Nociceptive sensitization, Insulin receptor, Diabetes, Sensory neurons, Hyperalgesia, *Drosophila*

INTRODUCTION

Drosophila has emerged as a useful system for the study of insulin signaling/diabetes and nociception. With respect to insulin signaling, flies have a canonical Insulin receptor (Insulin-like receptor, InR)

(Fernandez et al., 1995), a collection of *Drosophila* insulin-like peptides (Ilps) (Ikeya et al., 2002) manufactured by insulin-producing cells (IPCs) in the brain, and a downstream signal transduction cascade consisting of conserved components (Teleman, 2010). Dysregulation of Ilp production leads to a type 1-like diabetic state in *Drosophila* larvae (Rulifson et al., 2002), while a high-sugar diet leads to insulin resistance and a type 2-like diabetic state (Morris et al., 2012; Musselman et al., 2011; Skorupa et al., 2008). Together, insulin signaling and diabetic states in *Drosophila* regulate systemic glucose metabolism and organ-specific metabolic programs that impact muscle/cardiac function (Demontis and Perrimon, 2010; Na et al., 2013) and immunity (Musselman et al., 2017). However, whether diabetic larvae exhibit the types of sensory phenotypes often associated with diabetic patients remains unclear.

Drosophila is also a powerful model for nociception and nociceptive sensitization (Himmel et al.; Im and Galko, 2012). Many of the essential cell types and molecular players are conserved across phyla. At the cellular level, responses to noxious heat and noxious mechanical stimuli in larvae are detected by class IV multidendritic (md) neurons (Hwang et al., 2007), the dendrites of which tile over the barrier epidermis (Grueber et al., 2002) and the axons of which connect to a variety of functionally important second-order neurons in the larval ventral nerve cord (Hu et al., 2017; Yoshino et al., 2017; Ohyama et al., 2015). A number of conserved signaling pathways regulate tissue damage-induced nociceptive sensitization (Gold and Gebhart, 2010). In *Drosophila* larvae, these include Tumor necrosis factor (TNF; Egr) (Babcock et al., 2009), Hedgehog (Hh) (Babcock et al., 2011) and Substance P/Tachykinin (Tk) (Im et al., 2015). Whether baseline nociception (in the absence of injury) or injury-induced nociceptive sensitization is altered by disease-like states, such as diabetes, remains an open question in *Drosophila*.

Patients with diabetes often experience discomfiting alterations in sensory perception as the disease progresses (Veves et al., 2008). These changes often begin with nociceptive hypersensitivity to temperature and touch before progressing to numbness or hyposensitivity. There is substantial debate about the etiology of these diabetes-induced sensory alterations (Obrosova, 2009; Zochodne, 2016), including their relation to systemic glucose levels, diabetes-induced vascular changes, peripheral neurodegeneration or neuronal functions of insulin signaling (Gralle, 2017; Grote and Wright, 2016). More recently, evidence has emerged of sensory neuron intrinsic factors (Tsantoulas et al., 2017) and glucose toxicity affecting sensory perception of painful stimuli (Bierhaus et al., 2012; Orestes et al., 2013). Most vertebrate experimental models of the painful diabetic neuropathy involve either systemic pharmacological treatments or whole-animal genetic alterations (Obrosova, 2009). One unaddressed question is the relative contribution of various tissues, including peripheral sensory neurons, to painful sensory alterations. To date, there have been no models of diabetes-associated nociceptive changes that employ highly genetically tractable organisms such as *Drosophila*.

¹Department of Genetics, University of Texas MD Anderson Cancer Center, 1515 Holcombe Boulevard, Houston, TX 77030, USA. ²Neuroscience Institute, Georgia State University, P.O. Box 5030, Atlanta, GA 30303, USA. ³Genetics and Epigenetics Graduate Program, University of Texas Graduate School of Biomedical Sciences, 6767 Bertner Avenue, Houston, TX 77030, USA.

*Present address: Department of Biology, Haverford College, 370 Lancaster Avenue, Haverford, PA 19041, USA.

‡Authors for correspondence (seolheem@mdanderson.org; mjgalko@mdanderson.org)

© S.H.I., 0000-0002-0777-3466; D.N.C., 0000-0001-9191-9212; M.J.G., 0000-0002-3759-2017

This is an Open Access article distributed under the terms of the Creative Commons Attribution License (<http://creativecommons.org/licenses/by/3.0>), which permits unrestricted use, distribution and reproduction in any medium provided that the original work is properly attributed.

RESULTS

***InR* mutant larvae exhibit persistent thermal hyperalgesia**

To explore the possibility that larvae with alterations in insulin signaling might exhibit nociceptive phenotypes, we first tested whether *InR* mutant larvae exhibited changes in baseline thermal nociception and thermal hyperalgesia (increased sensitivity to noxious thermal stimuli), using assays standard in the field (Chattopadhyay et al., 2012) (Fig. 1A,B). Because homozygous *InR* loss-of-function mutants are larval lethal (Chen et al., 1996), we tested larvae heterozygous for two hypomorphic alleles of *InR* (*InR^{e19}*, *InR^{93Dj4}*), and larvae transheterozygous for the two alleles (*InR^{e19/93Dj4}*) (Tatar et al., 2001). These larvae had a normal number

of responders during baseline thermal nociception in response to a noxious stimulus (43°C) in the absence of injury (Fig. 1C), although there was a difference in the average latency of the responders for the *InR^{93Dj4/+}* and *InR^{e19/93Dj4}* alleles (Fig. S1). After UV-induced tissue injury (Babcock et al., 2009), both control and *InR* mutant larvae showed a normal acute thermal hyperalgesia response at 8 h post-injury when tested at this same temperature (Fig. 1D). However, in *InR* mutants, this acute sensitization failed to resolve over the normal time course (Fig. 1E), and continued as persistent thermal hyperalgesia at a time (24 h post-injury) when acute sensitization has resolved in controls. The persistent thermal hyperalgesia phenotype is significant in *InR* heterozygotes and is

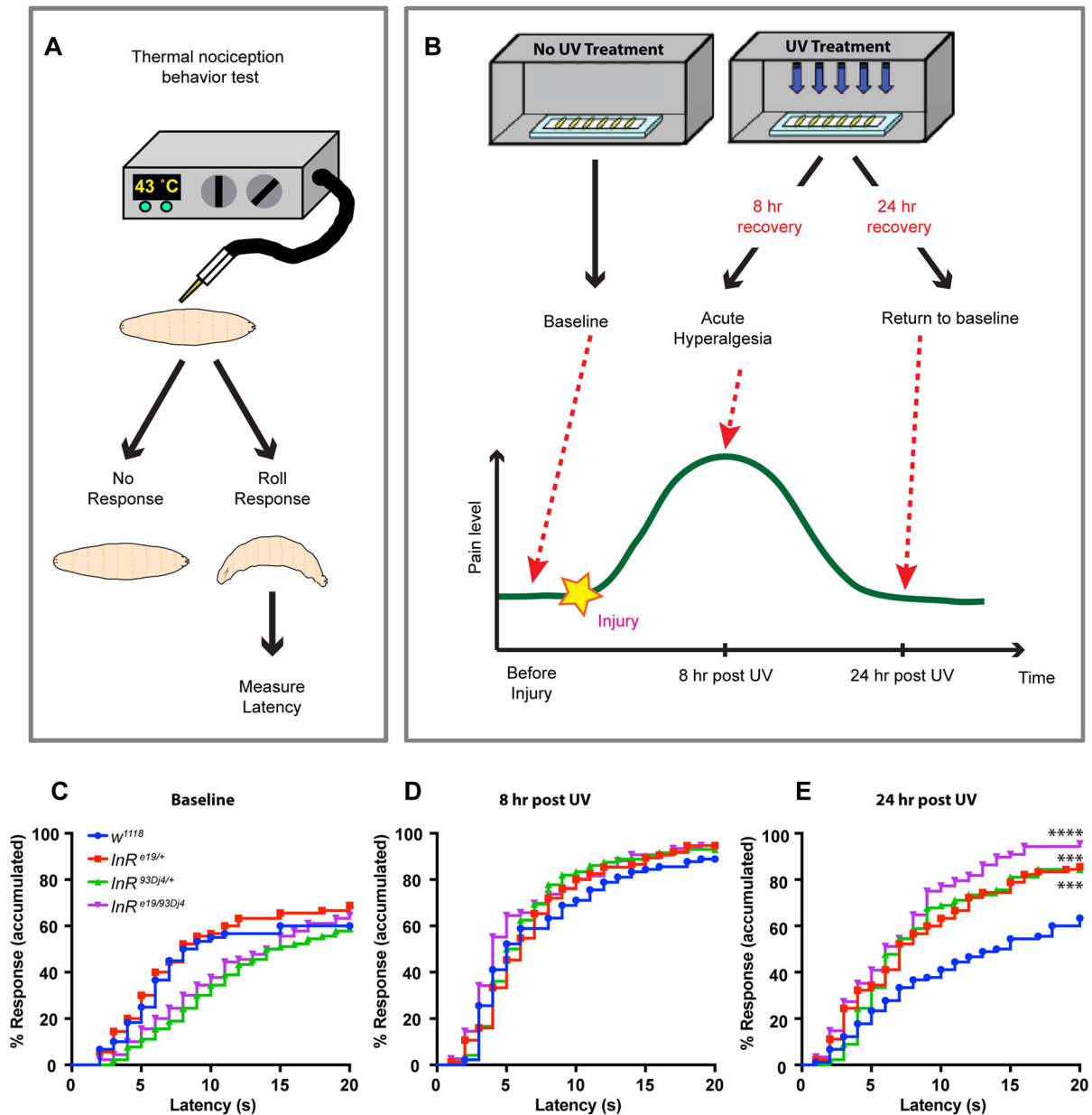


Fig. 1. *InR* mutant larvae exhibit persistent thermal hyperalgesia. (A,B) Schematics of the nociception (A) and persistent nociceptive sensitization (B) assays. (C-E) Quantitation of nociceptive behavioral responses to thermal stimulation at 43°C of *InR* mutant larvae. *w¹¹¹⁸* control larvae, two heterozygous hypomorphic alleles and a transheterozygous allelic combination of *InR* were tested: *InR^{e19/+}*, *InR^{93Dj4/+}*, *InR^{e19/93Dj4}*. Baseline responses without UV tissue damage ($n=60$ for *w¹¹¹⁸*, $n=90$ for others) (C), thermal sensitivity at 8 h post-UV ($n=90$ for *w¹¹¹⁸*, $n=80$ for *InR^{e19/+}*, $n=88$ for *InR^{93Dj4/+}*, $n=76$ for *InR^{e19/93Dj4}*) (D), thermal sensitivity at 24 h post-UV ($n=88$ for *InR^{e19/93Dj4}*, $n=90$ for others) (E). Statistical significance was determined by the Log-rank test. **** $P<0.0001$, *** $P<0.001$.

more severe in the transheterozygous larvae (Fig. 1E). Therefore, whole-animal *InR* mutant larvae exhibit persistent thermal hypersensitivity, a phenotype reminiscent of the early phase of painful diabetic neuropathy.

Type 1 diabetic larvae exhibit persistent thermal hyperalgesia after injury

To determine whether the persistent thermal hyperalgesia observed in *InR* mutant larvae might be related to diabetes-induced sensory changes, we utilized both type 1 and type 2 diabetes models (Musselman et al., 2011; Rulifson et al., 2002). To create a type 1 diabetes-like state (Fig. 2A), we silenced insulin-producing cells (IPCs) by expressing an inward rectifying potassium channel (*Kir2.1*) using the *dilp2 (Ilp2)-Gal4* driver, which is specific for IPCs (Rulifson et al., 2002). Expression of *Kir2.1* in these cells results in a lack of circulating *Drosophila* insulin-like peptides 2, 3 and 5 (*Ilp2, 3, 5*) (Park et al., 2014). Morphologically, silencing of

IPCs in the absence of UV-induced injury did not significantly reduce the number of branches or total dendritic length of class IV neurons compared with *Gal4* alone controls, although it was significant against *UAS* alone controls. Type 1 diabetic larvae when UV irradiated exhibited a reduction in number of branches and total dendritic length compared with irradiated *Gal4* and *UAS* alone controls (Fig. 2B-D). Behaviorally, the baseline (absence of injury) nociceptive sensitivity of type 1 diabetic larvae at 43°C was similar to that of the *Gal4* and *UAS* alone control larvae (Fig. 2E). Similarly, both controls and type 1 diabetic larvae showed similar responses to a 43°C probe at the peak hyperalgesia time point (Fig. 2F) following UV-induced tissue injury. By contrast, we found that the type 1 diabetes-like state resulted in persistent hypersensitization. Control larvae invariably resolved their thermal hyperalgesia by 24 h following injury (Fig. 2G). Type 1 diabetic larvae, by contrast, still exhibited thermal hyperalgesia at this time (Fig. 2G). Therefore, a type 1 diabetes-like condition results in

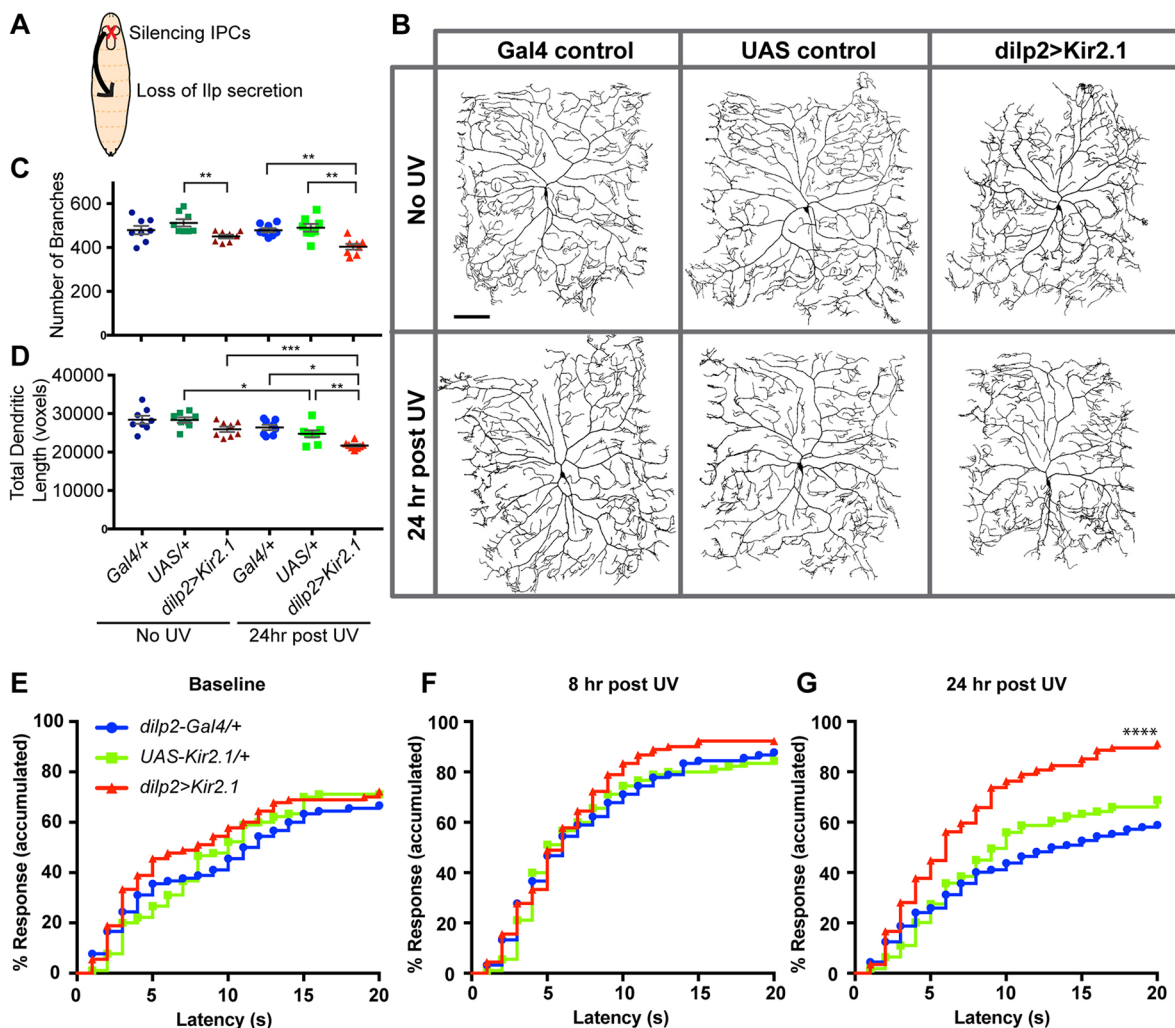


Fig. 2. A type 1 diabetes-like state induces persistent thermal hyperalgesia in *Drosophila* larvae. (A) Schematic of the genetic manipulation that induces a type 1 diabetes-like state in *Drosophila* larvae by silencing IPCs. (B) Representative *in vivo* confocal images of class IV md neuron dendritic morphology in controls and in larvae exhibiting a type 1 diabetes-like state±UV irradiation. In all panels, dendritic morphology was visualized using a *ppk-CD4::tdTomato* transgene. Controls: *dilp2-Gal4* alone and *UAS-Kir2.1* alone. Type 1 Diabetes: *dilp2-Gal4>UAS-Kir2.1*. (C,D) Quantitative dendritic morphology analysis measuring number of branches (C) and total dendritic length (D) presented as mean±s.e.m. $n=8$ neurons. Statistical significance was determined by one-way ANOVA with Bonferroni multiple comparison post hoc test. (E-G) Quantitation of nociceptive behavioral responses to thermal stimulation (43°C) in control larvae and when IPCs were silenced genetically. In all behavioral analyses, accumulated total responses were plotted as a function of latency to aversive withdrawal. Baseline behavioral responses in the absence of UV irradiation (E), thermal sensitivity at 8 h post-UV (F), thermal sensitivity at 24 h post-UV (G). $n=90$ larvae tested for each condition. * $P<0.05$, ** $P<0.01$, *** $P<0.001$, **** $P<0.0001$.

injury-induced persistent nociceptive hypersensitivity with no alteration in the baseline sensitivity or acute thermal hyperalgesia, similar to what is observed in *InR* mutants.

Type 2 diabetic larvae exhibit persistent thermal hyperalgesia after injury

To model type 2 diabetes (Fig. 3A), we cultured larvae on a high-sugar diet (Musselman et al., 2011). This nutritional regimen results in increased circulating sugar levels, fat accumulation and increased expression of *dilp* (*Ilp*) genes. Morphologically, the type 2 diabetic condition did not affect the number of dendritic branches in class IV md nociceptive neurons (Fig. 3B,C), although it did reduce the total dendritic length (Fig. 3B,D). No significant differences in morphological measures were observed with or without the high-sugar diet after UV-induced tissue injury (Fig. 3B-D).

Behaviorally, type 2 diabetic larvae did not exhibit any defects in baseline thermal nociception (43°C) (Fig. 3E) or in acute thermal hyperalgesia following UV-induced tissue injury (Fig. 3F). To test

whether there is developmentally induced shift in the timing or duration of the hyperalgesic peak, we examined larvae 16 h after injury. Control larvae had returned to baseline, as observed before (Babcock et al., 2009), whereas larvae grown on the high-sugar diet remained hypersensitive (Fig. 3G), a condition that persisted 24 h after irradiation (Fig. 3H). Taken together, we found that *Drosophila* larvae with a type 2 diabetes-like state exhibited a highly specific phenotype of persistent thermal hyperalgesia without corresponding defects in baseline thermal nociception or injury-induced acute thermal hyperalgesia.

Sensory neuron-specific loss of Insulin receptor causes persistent thermal hyperalgesia

The persistent thermal hyperalgesia in *InR* mutants and diabetic larvae suggest that insulin signaling is required to regulate the persistence of acute thermal nociceptive hypersensitivity. We thus asked in which tissue(s) InR function is required for diabetes-associated nociceptive persistence. To address this question, we

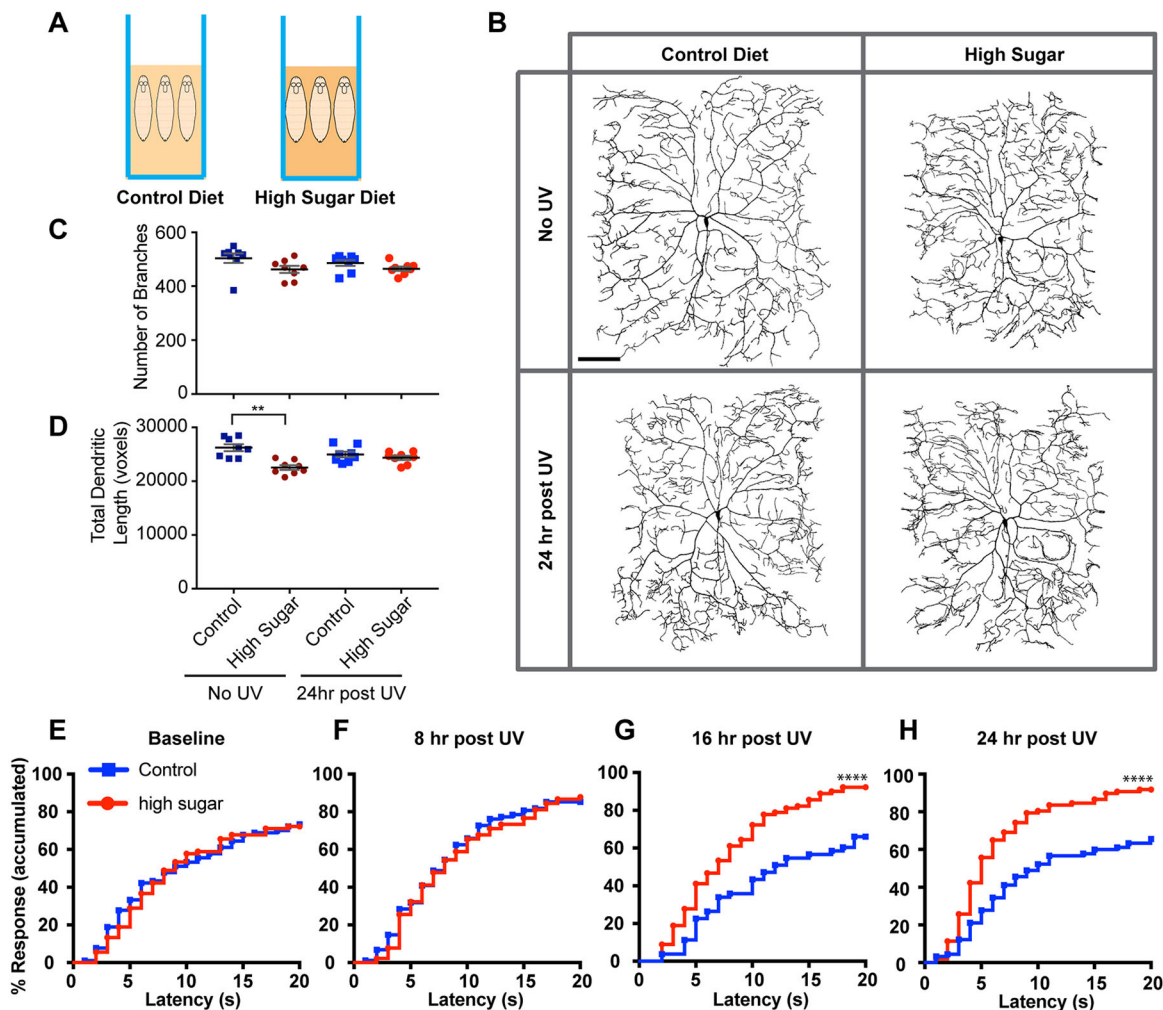


Fig. 3. A type 2 diabetes-like state induces persistent thermal hyperalgesia in *Drosophila* larvae. (A) Schematic of the diet condition (high sugar) that induces a type 2 diabetes-like state in exposed larvae. (B) Representative *in vivo* confocal images of class IV md neuron dendritic morphology in controls (normal diet) and in larvae exhibiting a type 2 diabetes-like state (high-sugar diet) ± UV irradiation. Dendritic morphology was visualized using a *ppk-CD4::tdTomato* transgene. (C,D) Quantitative dendritic morphology analysis measuring number of branches (C) and total dendritic length (D) presented as mean ± s.e.m. $n=8$ neurons. Statistical significance was determined by one-way ANOVA with Bonferroni multiple comparison post hoc test. (E-H) Quantitation of nociceptive behavioral responses to thermal stimulation (43°C) in control larvae and larvae fed a high-sugar diet. Baseline responses in the absence of UV irradiation ($n=90$ for each condition) (E), thermal sensitivity at 8 h post-UV ($n=88$ for control, $n=90$ for high sugar) (F), thermal sensitivity at 16 h post-UV ($n=53$ for control, $n=90$ for high sugar) (G), thermal sensitivity at 24 h post-UV ($n=90$ for control, $n=97$ for high sugar) (H). ** $P<0.01$, **** $P<0.0001$.

utilized tissue-specific Gal4 drivers (Table S1) to express a *UAS-InR^{RNAi}* transgene targeting *InR*. We then tested whether persistent thermal hyperalgesia was observed in progeny larvae expressing the *UAS-InR^{RNAi}* transgene in each tissue compared with relevant genetic controls (Gal4 transgenes alone). Larvae with muscle-, fat body- and hemocyte-specific Gal4 expression of *UAS-InR^{RNAi}* did not exhibit persistent thermal hyperalgesia (Fig. S2).

As *InR* function was not centered in typical metabolic control tissues, we tested sensory neurons themselves. Expression of *UAS-InR^{RNAi}* using a pan-md sensory neuron driver did not cause defects in baseline (Fig. 4A) or acute thermal hyperalgesia (Fig. 4B). By contrast, md neuron expression of *UAS-InR^{RNAi}* did result in prolonged thermal hyperalgesia that was apparent 24 h post-injury (Fig. 4C) and worsened throughout the third larval stage (Fig. 4D). These results indicate that perturbing *InR* function within multidendritic nociceptive sensory neurons, but not within other tissues that typically control metabolic regulation, leads to persistent thermal hyperalgesia following injury.

Specificity to peripheral nociceptive sensory neurons is supported because we also observed persistent thermal hyperalgesia with an independent pan-md driver and a class IV nociceptive sensory neuron md driver (Table S1, Figs S3 and S4). Independent *UAS-InR^{RNAi}* transgenes targeting nonoverlapping regions of *InR* (Fig. 4A-C; Fig. S5) gave the same phenotype, as did a *UAS-InR^{DN}* transgene (Wu et al., 2005) expressing a dominant negative form of *InR* (Fig. S6), ruling out RNAi off-target effects. RNAi transgenes targeting other components of the insulin-like signaling (ILS) pathway (*chico*, *Pi3K* genes) also resulted in persistent thermal hyperalgesia (Fig. S7).

Morphologically, md neuron-specific expression of *UAS-InR^{RNAi}* did not affect the total number of branches of class IV md neurons under baseline conditions, although it did reduce the total dendritic length (Fig. 4E-G). This pattern of morphological changes is similar to what was observed in the type 2 diabetic condition (Fig. 3B-D). However, with *UAS-InR^{RNAi}* expression in md neurons, there was a significant increase in the number of class IV dendritic branches after UV irradiation (Fig. 4E,F) that was not accompanied by a corresponding increase in total dendritic length (Fig. 4E,G). The relationship between the consistent behavioral phenotype and the relatively modest morphological changes across different genotypes and diabetic conditions is discussed further below.

Persistent thermal hyperalgesia is associated with elevated calcium responses in class IV nociceptive neurons

Is the behavioral hypersensitivity seen upon loss of *InR* in nociceptive sensory neurons accompanied by cellular level changes in neuronal activity? To assess this, we tried to use GCaMP (Chen et al., 2013) expressed within sensory neurons, but found that the GFP fluorescence was not stable over the duration of the noxious heat exposure (data not shown). As an alternative, we expressed CaMPARI (Fosque et al., 2015), a genetically encoded calcium integrator that undergoes fluorescence conversion from green to red as a function of high intracellular calcium and photoconverting (PC) light, in md neurons with or without *UAS-InR^{RNAi}*. Progeny larvae (control and *InR* loss of function) were mock irradiated or UV irradiated as in our behavioral analysis, and both groups were either challenged with a 43°C heat probe stimulus or not (see Materials and Methods, Fig. 5A for experimental flowchart). In the absence of PC light, the ratio of F_{Red}/F_{Green} (CaMPARI response) is low under all conditions tested, as expected (Fig. 5B, no PC). Exposure to PC light led to a slight (but not significant) increase in the CaMPARI response with or without UV

irradiation (Fig. 5B, PC, no stimulation). In control larvae, adding a noxious heat stimulus (43°C heat probe) with or without UV-induced injury did not significantly increase the observed CaMPARI response (Fig. 5B, compare PC, no stimulation controls with PC, stimulation controls). For *UAS-InR^{RNAi}*-expressing larvae, exposure to a noxious stimulus by itself was not sufficient to cause a significant increase in the CaMPARI response compared with controls (Fig. 5B, PC, stimulation). By contrast, *UAS-InR^{RNAi}*-expressing larvae that were UV irradiated and exposed to a noxious heat stimulus showed a significant increase in CaMPARI responses compared with all other relevant conditions (Fig. 5B, PC, stimulation). Representative neuronal cell bodies reflecting the average CaMPARI responses are depicted in Fig. 5C. Together, these results suggest that a significant increase in neuronal calcium is apparent when UV-induced tissue injury is combined with heat stimulation. Similar to our behavioral results, this increase at 24 h postirradiation is only seen when *InR* function is reduced in md neurons.

Constitutive activation of *InR* causes hyposensitivity during the acute phase

Our genetic analysis suggests that ILS might be required within md neurons to actively shut off acute thermal sensitization. To test this possibility we overexpressed a constitutive active (CA) form of *InR* (*UAS-InR^{CA}*) (Wang et al., 2008) in md neurons. If ILS is a general regulator of nociceptive sensation, we might expect constitutive activation of this pathway to alter baseline nociception in the absence of injury. This was not observed – *InR^{CA}* expression did not alter baseline (no injury) thermal nociception (43°C) (Fig. 6A). However, the acute thermal hyperalgesia, which peaked at 8 h after UV-induced injury in controls, was greatly attenuated in *UAS-InR^{CA}*-expressing larvae, even dipping below the normal nociceptive response to the 43°C stimulus (Fig. 6B). When examined at the normal recovery time point (24 h after injury) there were no sensitivity differences between *UAS-InR^{CA}*-expressing and relevant control larvae (Fig. 6C). Therefore, constitutive *InR* activation causes acute hyposensitivity after injury. Baseline nociception was not affected and the injury-induced hyposensitivity resolved with similar kinetics compared with the normal injury-induced hypersensitivity.

Multidendritic neuron-specific restoration of ILS rescues persistent nociceptive hypersensitivity

The finding that md neuron-specific loss causes persistent thermal hyperalgesia suggests that normal ILS is required in md neurons to successfully turn off injury-induced acute sensitization. The dampening of acute thermal hyperalgesia upon constitutive activation of ILS supports this idea. To further test this hypothesis we attempted to rescue ILS function in md sensory neurons both in *InR* mutants and in type 2 diabetic larvae. We expressed a *UAS-InR* transgene specifically in md neurons in a heterozygous *InR^{e19}* background and tested the resulting larvae for thermal sensitization versus relevant genetic controls. There were no differences in baseline thermal nociception (Fig. 7A) or acute thermal hyperalgesia (Fig. 7B) between the rescued larvae and the controls. However, at the recovery time point, we found that larvae expressing *UAS-InR* in their nociceptive sensory neurons showed a normal recovery, whereas control larvae (Gal4 or *UAS* transgene alone) lacking *InR* expression still showed persistent thermal hyperalgesia (Fig. 7C). We also found that constitutively activating *InR* in nociceptive sensory neurons of type 2 diabetic larvae did not affect baseline nociception (Fig. 7D), but caused hypoalgesia at the acute time point (Fig. 7E) coupled with a normal

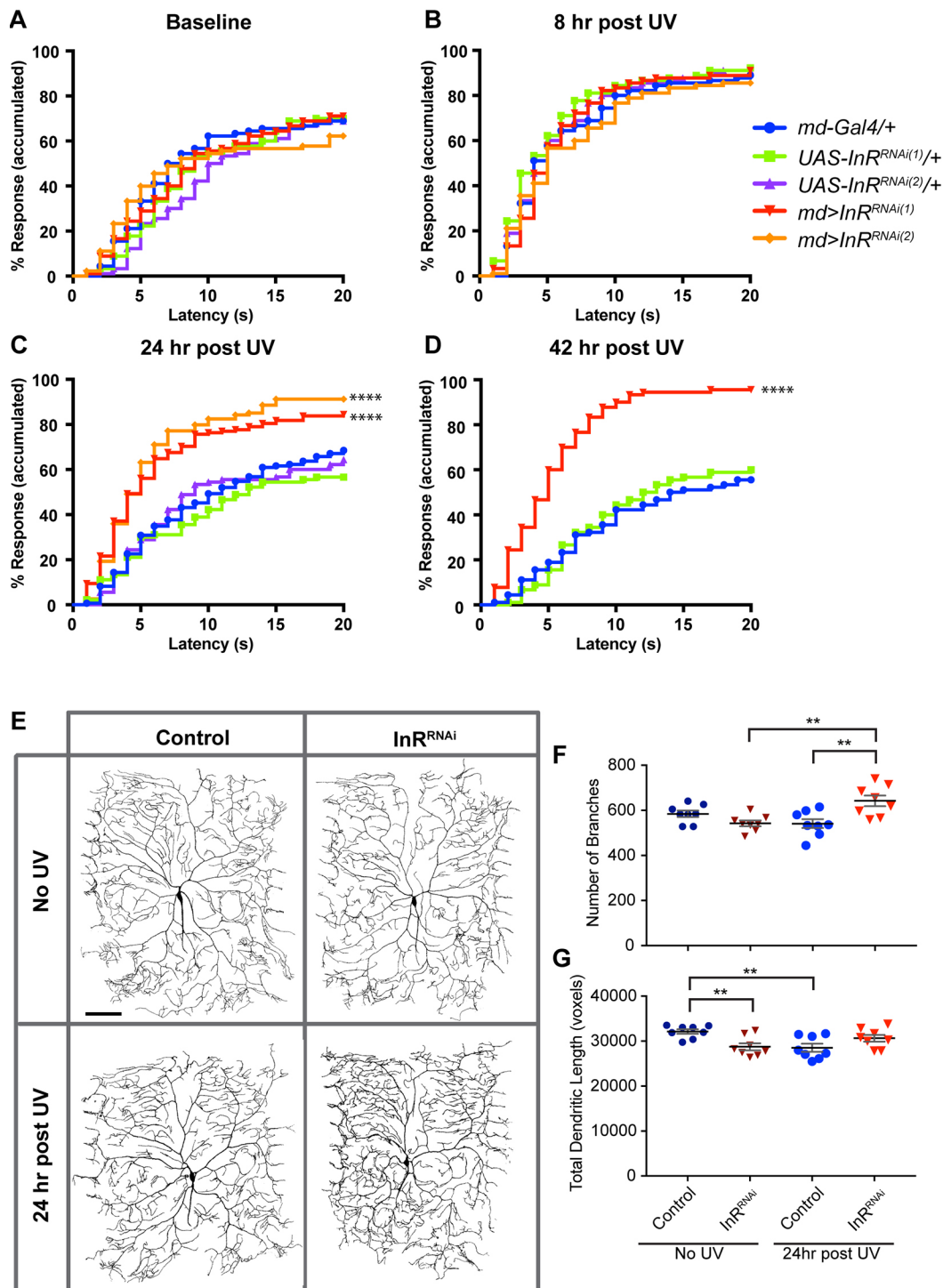


Fig. 4. Sensory neuron-specific interference with InR function causes persistent thermal hyperalgesia. (A–D) Quantitation of thermal nociceptive behavioral responses (43°C) when *UAS-InR^{RNAi}* is expressed in md neurons. $n=90$ for each condition. Baseline responses in the absence of UV irradiation (A), thermal sensitivity at 8 h post-UV (B), thermal sensitivity at 24 h post-UV (C), thermal sensitivity at 42 h post-UV (D). (E) Representative *in vivo* confocal images of class IV md neuron dendritic morphology labeled with *ppk1.9-GAL4,UAS-mCD8::GFP*. Dendritic morphology was compared between control larvae expressing *UAS-Luc^{RNAi}* and larvae expressing *UAS-InR^{RNAi}±UV* irradiation. (F,G) Quantitative dendritic morphology analysis measuring number of branches (F) and total dendritic length (G) presented as mean±s.e.m. $n=8$ neurons. Statistical significance was determined by one-way ANOVA with Bonferroni multiple comparison post hoc test. ** $P<0.01$.

recovery to baseline at 24 h (Fig. 7F). Together, these results support the hypothesis that the function(s) of InR relevant to regulating nociceptive sensitivity following injury or induction of a diabetic state lie mainly within nociceptive sensory neurons.

DISCUSSION

Our results suggest that InR function in nociceptive md sensory neurons is important to regulate the persistence of injury-induced nociceptive sensitization (Fig. 8). *InR* mutants exhibit a highly

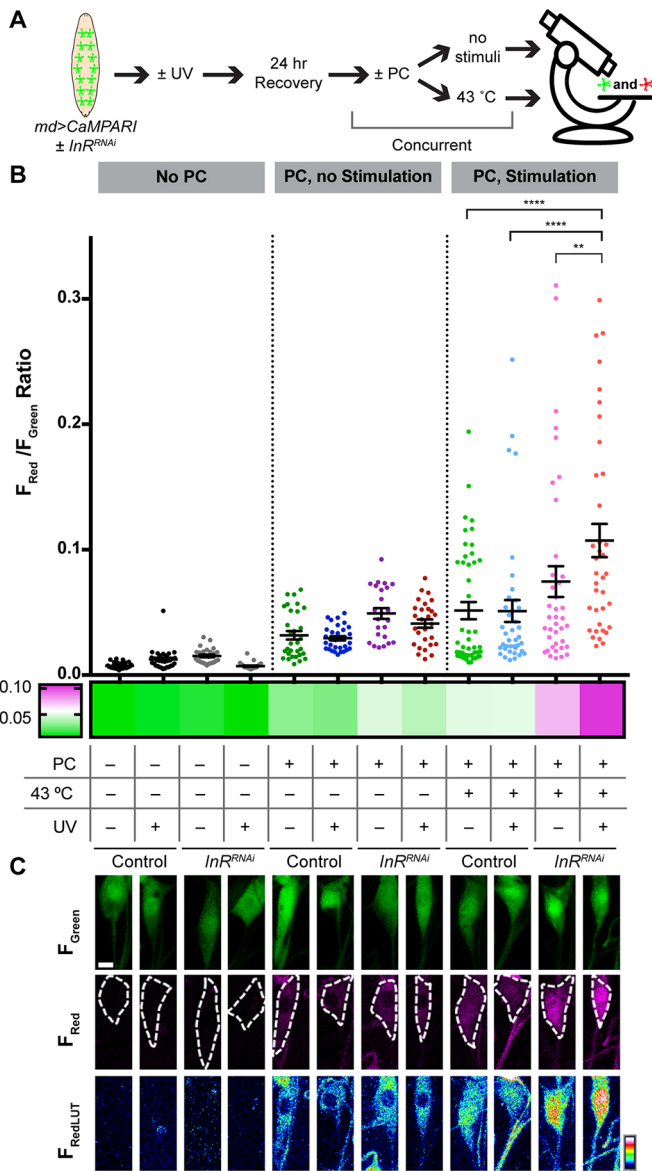


Fig. 5. CaMPARI analysis reveals increased cellular calcium in sensory neurons. (A) Schematic of CaMPARI experimental outline. (B) Quantitative analysis of CaMPARI responses in class IV md neurons of larvae expressing *UAS-CaMPARI* via *md-Gal4±UAS-InR^{RNAi}*. The CaMPARI response is calculated as the F_{Red}/F_{Green} ratio presented as mean±s.e.m. and is represented graphically, where each measured neuron is represented by a single data point, and also as a heatmap depicting the averaged CaMPARI response. On the heatmap, magenta indicates a higher F_{Red}/F_{Green} ratio and green indicates a lower ratio. $n=24-45$ neurons. Statistical significance was determined by one-way ANOVA with Bonferroni multiple comparison post hoc test. A key to relevant experimental variables (PC light, thermal stimulation, UV and genotype) is provided and applies to the quantitative data in B and the micrographs in C. (C) Representative *in vivo* confocal images of class IV md neuronal cell bodies. For each condition the F_{Green} , F_{Red} and F_{RedLUT} (a heatmap representation of photoconverted CaMPARI intensity) are shown. $**P<0.01$, $****P<0.0001$.

specific phenotype whereby baseline nociception and the normal acute nociceptive sensitization response are unaffected. In *InR* mutant larvae, however, the acute response does not resolve back to baseline, resulting in persistent sensitization. An md neuron-intrinsic function of InR is supported by four lines of evidence: (1) md neuron-specific loss of InR function leads to persistent

thermal hyperalgesia; (2) md neuron-specific loss of InR function leads to increased neuronal calcium responses at a time point consistent with behavioral hypersensitivity; (3) md neuron-specific restoration of InR rescues persistent thermal hyperalgesia observed in *InR* mutants; and (4) md neuron-specific constitutive activation of InR dampens the peak of acute injury-induced hyperalgesia. These results suggest that InR function might become active during the recovery phase of sensitization – a conclusion supported by the specific dampening of the acute thermal hyperalgesia response in nociceptive sensory neurons expressing constitutively active InR.

Our results also suggest that the md neuron-specific role of InR might be relevant to diabetes-associated nociceptive phenotypes. First, larvae experiencing both type 1 and type 2 models of diabetes exactly phenocopy the loss of InR in md neurons – persistence of thermal hypersensitivity. Second, md neuron-specific rescue of InR function can ameliorate the persistent thermal hyperalgesia seen in both *InR* mutants and in type 2 diabetic larvae. Below, we discuss the possible implications of these findings in flies and in other models of diabetes-associated pain.

InR has diverse functions in multiple tissues so that each tissue can be responsive to the organism's metabolic state (Demontis and Perrimon, 2010; Wessells et al., 2004). The relevant tissue for the regulation of nociception is not clear. Our data suggest that the activity of InR relevant to nociceptive sensitization is not localized in the major metabolic signaling tissues of the fly larva – fat body, muscle or hemocytes. Rather, InR functions in the very sensory neurons that respond to noxious thermal stimuli. In vertebrates, the insulin receptor is expressed on nociceptive sensory neurons (Sugimoto et al., 2002, 2000), but whether it functions in nociceptive sensory neurons has not been tested to date. Further, the conditional InR knockouts generated to date have not been tested for pain phenotypes (Bruning et al., 2000). However, mouse insulin receptor can regulate synapse number and neuronal plasticity, at least in central nervous system neurons (Chiu et al., 2008; Grillo et al., 2015). Given that nociceptive biology is evolutionarily conserved, our work suggests that it would be interesting to test pain physiology in a nociceptor-specific knockout of the mouse insulin receptor.

With InR loss of function we observe cellular-level changes – increased cellular calcium measured by CaMPARI and modest changes in dendritic morphology – that could conceivably help explain the observed behavioral hypersensitivity. As a genetically encoded calcium integrator, CaMPARI allows for post hoc assessment of neural activation states as a function of stimulus conditions and in combination with genetic perturbations. Previous studies have utilized CaMPARI to measure *in vivo* neuronal activity levels in response to a broad range of sensory stimuli in *Drosophila*, zebrafish and mice (Enjin et al., 2016; Fosque et al., 2015; Turner et al., 2016), as well as in mapping functional synaptic connectivity (Zolnik et al., 2017). In the case of InR function assessed here, CaMPARI analysis indicates increased md neuron function/output at the time when hypersensitivity would have resolved in control larvae. The observed morphology changes, which are modest but significant, are not uniform across diabetic conditions (type 1 and type 2) and genetic manipulations (md neuron-specific expression of *InR^{RNAi}*). However, the observed behavioral phenotype – persistent thermal hyperalgesia – is shared across all conditions. For this reason, we suspect that morphological changes at the dendritic level are unlikely to be a major driver of the behavioral phenotype. The morphological changes observed are consistent with the peripheral neurotogenic effects of insulin observed in vertebrate neuronal culture (Ferynhough et al., 1993; Recio-Pinto et al., 1986).

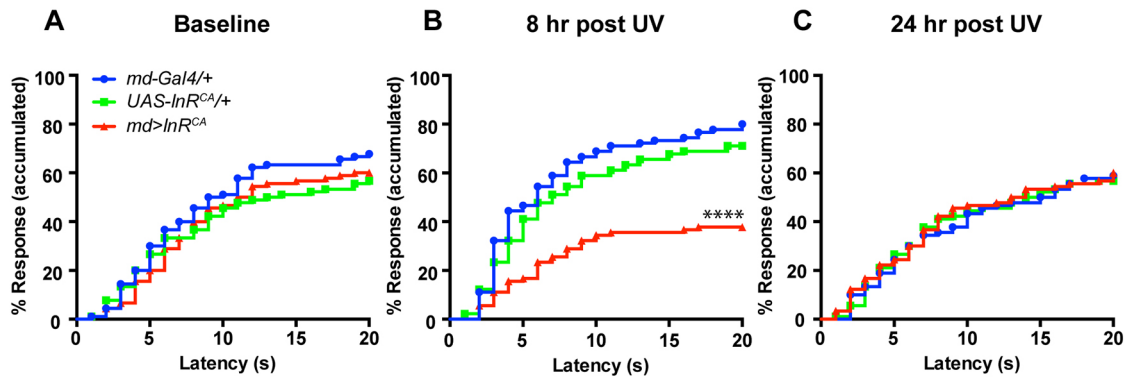


Fig. 6. Constitutive activation of InR causes hyposensitivity during the acute phase. (A-C) Quantitation of thermal nociceptive behavioral responses (43°C) when *UAS-InR^{CA}* is expressed in md neurons versus Gal4 and UAS alone controls. Baseline responses in the absence of UV irradiation (A), thermal sensitivity at 8 h post-UV (B), thermal sensitivity at 24 h post-UV (C). $n=90$ for each condition/genotype. **** $P<0.0001$.

An important question is when ILS is activated following injury. Given that *InR* loss of function results in persistent thermal hyperalgesia following a normal peak of acute hyperalgesia, it seems likely that ILS would be activated after the acute response. The normal thermal nociception baseline and the acute thermal hyposensitivity observed upon constitutive activation of InR are consistent with this idea. There is precedence in *Drosophila* for UV injury increasing ILS in non-neuronal tissues (Karpac et al., 2011). If ILS were activated neuronally after the peak of acute hyperalgesia, this could in turn dampen injury-induced hypersensitivity and help the acute response return to baseline. Consistent with this idea, pre-activating ILS (constitutive activation of InR) temporally shifts the dampening of nociceptive sensitivity from the recovery time point

(24 h) to the peak time point (8 h). Comparing the timing and magnitude of sensitivity between *InR^{RNAi}*- and *InR^{CA}*-expressing larvae, the most likely time of activation of ILS following injury is during the normal recovery phase (Fig. 8).

Several models could potentially account for how InR regulates the persistence of acute sensitization. One model, consistent with our experiments with activation of InR and the timing of ILS activation, is that ILS helps shut off the acute nociceptive sensitization response. This model predicts some crosstalk between ILS and acute sensitization pathways, such as TNF, Tachykinin or Hedgehog, and/or the downstream TRP channels through which these sensitization pathways act (Babcock and Galko, 2009; Babcock et al., 2011; Im et al., 2015). Hedgehog

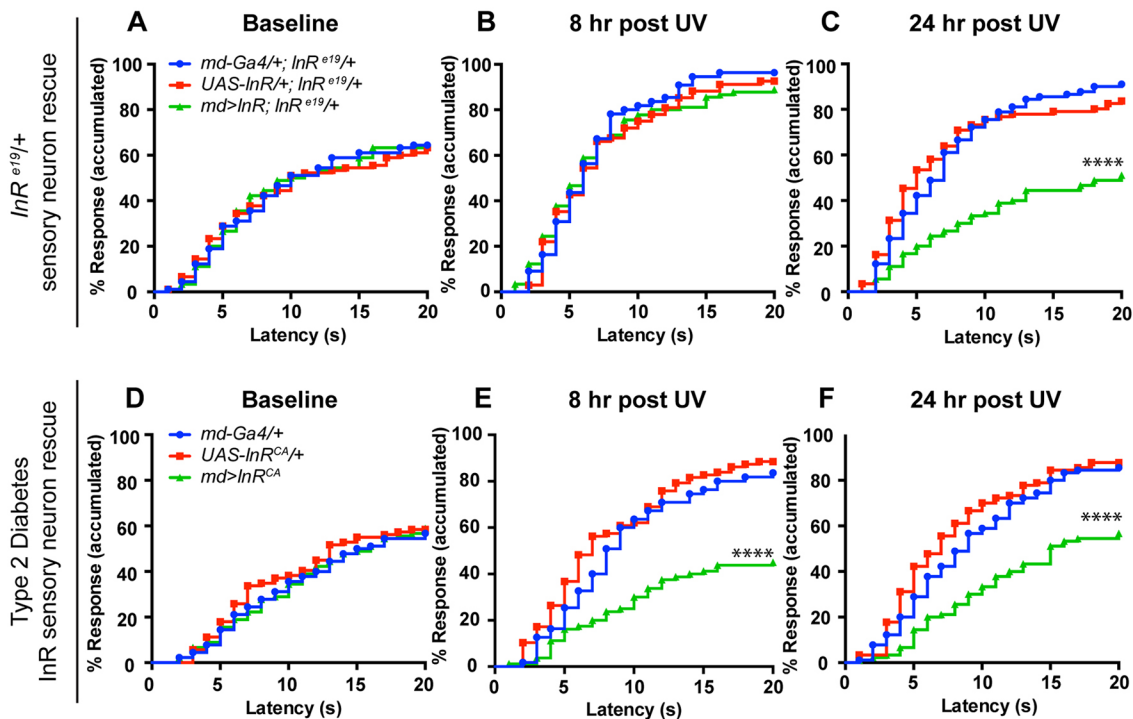


Fig. 7. Expression of InR in md neurons rescues the persistent thermal hyperalgesia of *InR* mutants and type 2 diabetic larvae. (A-C) Quantitation of nociceptive behavioral responses (43°C) when *UAS-InR* is expressed in md sensory neurons in the heterozygous *InR* mutant background. Baseline responses without UV irradiation (A), UV-induced acute hyperalgesia (8 h post-UV) (B), UV-induced persistent hyperalgesia (24 h post-UV) (C) ($n=90$ for each condition/genotype). (D-F) Quantitation of nociceptive behavior responses (43°C) when *UAS-InR^{CA}* is expressed in md sensory neurons in the high-sugar fed larvae. Baseline responses without UV irradiation ($n=90$) (D), UV-induced acute hyperalgesia (8 h post-UV) ($n=55$ for Gal4 alone, $n=87$ for UAS alone, $n=80$ for *md>InR^{CA}*) (E), UV-induced persistent hyperalgesia (24 h post-UV) ($n=90$) (F). **** $P<0.0001$.

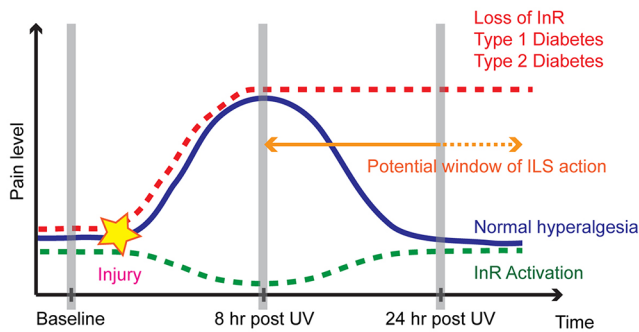


Fig. 8. Graphical representation of pain levels versus time postinjury, annotated across control, persistently hypersensitive genotypes and diabetic conditions, and upon constitutive activation of InR. Control, blue solid line; persistently hypersensitive genotypes and diabetic conditions, red dashed line; constitutive activation of InR, green dashed line. Landmark time points (gray vertical bars) and the likely window of ILS activity in nociceptive sensory neurons (orange arrow/text) are indicated.

signaling, because it is required for acute hyperalgesia (Babcock et al., 2011) and regulates metabolic effects (Rodenfels et al., 2014), seems a plausible target of ILS. A second model is that ILS effects could be more direct – insulin can affect TRPV1 sensitivity and membrane levels (Lilja et al., 2007) in some neurons. A third model postulates that ILS, once it is activated post-injury, turns on novel regulators of neuronal firing that counteract the effects of acute sensitization pathways (Augustin et al., 2017). Such regulators might include the HCN2 channel, which regulates nociceptive sensitivity during diabetic neuropathy (Tsantoulas et al., 2017) and/or GRK2, which regulates duration of acute sensitization responses (Wang et al., 2011).

Our finding that both type 1 and type 2 larval models of diabetes phenocopy sensory neuronal loss of InR suggests strongly that there is a tie to diabetes-associated pain. The persistent sensitization observed in type 1 and type 2 larval models demonstrate that, at least in principle, diabetic states can alter the behavioral response(s) mediated by sensory neurons over a highly compressed timescale and without dramatic changes to the morphology of distal terminals. This might be most relevant to the early phases of painful diabetic neuropathy that are characterized by sensory hypersensitivity, often in the absence of overt neuronal morphology changes (Wright et al., 2007). The later phase of painful diabetic neuropathy, often associated with sensory numbness, is correlated with peripheral neuronal degeneration (Kennedy et al., 1996). Is the sensory hypersensitivity phenotype observed under diabetic conditions related to hyperglycemia or insulin resistance? Tight glycemic control does not necessarily track well with pain symptoms in patients (Chan et al., 1990). Further, a number of prior studies have suggested that diabetic neuropathy can be separated from hyperglycemia (Brussee et al., 2004; Romanovsky et al., 2010). Nociceptive sensory neurons, which express the insulin receptor (Sugimoto et al., 2002, 2000), can become insulin resistant both in culture (Kim et al., 2011) and under diabetic conditions (Grote et al., 2013). These data, together with our own data supporting a nociceptor-localized role for ILS in controlling nociceptive duration, suggest that nociceptors themselves are a functionally relevant tissue for insulin action during regulation of nociception.

Our work establishes a novel genetically tractable model of neuronal InR function and diabetes-associated nociceptive changes. Such fly models can serve as hypothesis generators for complementary vertebrate approaches, as well as a platform for

future gene discovery approaches (Bellen et al., 2010; Graham and Pick, 2017). One implication of our work is that diabetes-associated nociceptive changes might be more injury dependent and closely related to the acute-to-chronic switch associated with standard injury-dependent sensitization than previously appreciated. A second implication is that diabetes-associated changes in nociception could be more driven by primary changes in ILS, as opposed to secondary effects on associated tissues such as the vasculature (Powell et al., 1985). Future work on this model and testing logical hypotheses emerging from this model in vertebrate systems will determine how relevant the model is, given the added complexity of diabetes-associated sequelae and nociceptive circuitry in vertebrates.

MATERIALS AND METHODS

Fly stocks and genetics

Stocks were obtained from the Bloomington *Drosophila* Stock Center (NIH P400D018537) and the Vienna *Drosophila* RNAi Center. All experimental crosses were performed at 25°C, with the exception of *InR* transheterozygotic combination (*InR*^{19/93Dj4}) (Tatar et al., 2001), which was reared at 18°C until third instar larval stage and then moved to 25°C for experiments. Flies were raised on regular corn meal media except for the type 2 diabetes experiments. A high-sugar diet (10 g/l agar, 80 g/l brewer's yeast, 20 g/l yeast extract, 20 g/l peptone, 342 g/l sucrose, 0.5 g/l MgSO₄, 0.5 g/l CaCl₂, 6 ml/l propionic acid, 0.1% mold inhibitor) contains 6.7 times higher sugar compared with a control diet (51 g sucrose, all other ingredients the same) (Musselman et al., 2011). *w*¹¹¹⁸ and/or *Gal4*^{109(2)80/+} (crossed to *w*¹¹¹⁸) served as control strains for behavioral analysis and staining. *InR* mutant alleles used were *InR*¹⁹ and *InR*^{93Dj4}. Tissue-specific expression of *UAS* transgenes was controlled by *Gal4*¹⁰⁹⁽²⁾⁸⁰ (Gao et al., 1999) or *21-7-Gal4* (Song et al., 2007) for all four classes of md neurons, *ppk1.9-Gal4* for class IV md neurons (Ainsley et al., 2003), *dilp2-Gal4* for IPCs (Rulifson et al., 2002), *hmlA-Gal4* (Sinenko and Mathey-Prevot, 2004) for circulating hemocytes, *Dmef2 (Mef2)-Gal4* for muscle (Zars et al., 2000) and *OK376-Gal4* for larval fat body (Wu et al., 2009). *UAS-Kir2.1* was used to silence IPCs and block Ilp secretion (Kim and Rulifson, 2004). *UAS-InR^{DN}* (K1409A) (Wu et al., 2005), *UAS-InR^{CA}* (A1325D) (Wang et al., 2008) and *UAS-InR* (Martin-Pena et al., 2006) were used to manipulate InR function, and *UAS-CaMPARI* (Fosque et al., 2015) was used to monitor Ca²⁺ levels within class IV md neurons. RNAi lines (Dietzl et al., 2007; Ni et al., 2011) used were *InR*^{JF01482}, *InR*^{JF01183}, *chico*^{JF02964}, *Pi3K68D*^{GD7348}, *Pi3K92E*^{GD11228} and *Luc*^{JF01355}. Table S2 lists all of the specific genotypes used in each figure panel throughout the manuscript.

Behavioral assays

UV-induced tissue damage and thermal nociception assays were performed as described previously (Babcock et al., 2009; Chatopadhyay et al., 2012; Im et al., 2015), and a brief description follows. To induce tissue damage, early third instar larvae were etherized (Ethyl Ether Anhydrous, Thermo Fisher Scientific), immobilized and exposed to 254 nm wavelength UV at a setting of 20 mJ/cm² for ~5 s using spectrolinker XL-1000 UV crosslinker (Spectrolink). During irradiation, a hand-held UV spectrophotometer (AccuMAX XS-254, Spectrolink) was placed next to the specimen to read the exact UV dose – usually 11–14 mJ/cm². Mock or UV-irradiated larvae were returned to fly food until thermal nociception assays were performed. For the thermal nociception assay, a metal tip of a custom-built thermal probe, the surface temperature of which is fine-tuned, touches the dorsal side of an early third instar larva in abdominal segments A3–A5. All thermal nociception assays in this paper were performed at a heat probe setting of 43°C (Babcock et al., 2009). Thermal hyperalgesia assays were performed 8 h after UV irradiation. Persistent hyperalgesia assays were performed 24 h or 42 h after UV irradiation. Aversive withdrawal behavior (corkscrew-like rolling) was scored under a dissecting stereomicroscope and the latency was recorded up to a 20 s cutoff. Behavioral assays were performed in triplicate sets of 30 or more larvae, and accumulated total percent responses were plotted as a function of latency (duration of probe contact until initiation of

rolling). Statistical significance was tested using Log-rank analysis in GraphPad Prism unless noted otherwise in the figure legends.

Live imaging and confocal microscopy

Confocal imaging of *in vivo* neuronal morphology was performed as previously described (Das et al., 2017; Turner et al., 2016). Briefly, third instar larvae were mounted on slides with 1:5 (v/v) diethyl ether:halocarbon oil and imaged on a Zeiss LSM780 confocal system. Z-stacks of class IV md neurons were obtained and neuromorphometric analyses of two-dimensional maximum projections of the z-stacks were performed using Adobe Photoshop and ImageJ (Analyze Skeleton plug in: <http://imagej.net/AnalyzeSkeleton>) as previously described, with modification (Iyer et al., 2013). Statistical significance was tested using one-way ANOVA with Bonferroni multiple comparison post hoc test in GraphPad Prism.

CaMPARI analysis

CaMPARI imaging was performed as previously described (Patel and Cox, 2017; Turner et al., 2016) with the following modifications. Third instar control and *UAS-InR^{RNAi}* larvae expressing *UAS-CaMPARI* were analyzed in the presence or absence of photo-converting (PC) light (440 nm excitation), UV irradiation and/or a 43°C heat probe stimulus applied as in the behavioral experiments. Z-stack images were taken using a Zeiss LSM780 confocal system at 1024×1024 pixel resolution using a Plan-Apochromat 20×/0.8 NA and 1.4 digital zoom. 3D z-stacks were transformed to 2D maximum projection images and fluorescence intensity normalized to area for F_{Red} and F_{Green} was measured using Zen blue (Lite) from Zeiss. CaMPARI responses were recorded from class IV md neurons across abdominal segments A1-A4. Identical settings for laser intensity and other image capture parameters were applied for comparison of CaMPARI responses across conditions. Statistical significance was tested using one-way ANOVA with Tukey multiple comparison post hoc test in GraphPad Prism.

Acknowledgements

We thank Elizabeth Chen, Yuh Nung Jan, Ulrich Theopold and Kartik Venkatachalam for *Drosophila* stocks; members of the Galko laboratory for critical comments on the manuscript; Adriana Paulacci-Holthausen for assistance with confocal microscopy; and Cox laboratory members Jamin M. Letcher and Shatabdi Bhattacharjee for assistance with morphology analyses.

Competing interests

The authors declare no competing or financial interests.

Author contributions

Conceptualization: S.H.I., A.A.P., D.N.C., M.J.G.; Methodology: S.H.I., A.A.P., M.J.G.; Validation: D.N.C.; Formal analysis: S.H.I., A.A.P.; Investigation: S.H.I., A.A.P.; Resources: D.N.C., M.J.G.; Data curation: A.A.P.; Writing - original draft: S.H.I., M.J.G.; Writing - review & editing: S.H.I., A.A.P., D.N.C., M.J.G.; Visualization: S.H.I., A.A.P.; Supervision: D.N.C., M.J.G.; Project administration: D.N.C., M.J.G.; Funding acquisition: D.N.C., M.J.G.

Funding

This work was supported by National Institute of Neurological Disorders and Stroke (NINDS) (R01NS069828 to M.J.G.; R01NS086082 to D.N.C.); National Institute of General Medical Sciences (NIGMS) (R35GM126929 to M.J.G.); Office of Extramural Research, National Institutes of Health (T32-CA009299-34 to S.H.I.); Georgia State University (D.N.C.); 2CI Neurogenomics Fellowship and Kenneth W. and Georganne F. Honeycutt Fellowship to A.A.P.; and University of Texas MD Anderson Cancer Center (R. Lee Clark Fellowship to M.J.G.).

Supplementary information

Supplementary information available online at <http://dmm.biologists.org/lookup/doi/10.1242/dmm.034231.supplemental>

References

Ainsley, J. A., Pettus, J. M., Bosenko, D., Gerstein, C. E., Zinkevich, N., Anderson, M. G., Adams, C. M., Welsh, M. J. and Johnson, W. A. (2003). Enhanced locomotion caused by loss of the *Drosophila* DEG/ENaC protein Pickpocket1. *Curr. Biol.* **13**, 1557-1563.

Augustin, H., MCGourty, K., Allen, M. J., Madem, S. K., Adcott, J., Kerr, F., Wong, C. T., Vincent, A., Godenschwege, T., Boucrot, E. et al. (2017). Reduced insulin

signaling maintains electrical transmission in a neural circuit in aging flies. *PLoS Biol.* **15**, e2001655.

Babcock, D. T. and Galko, M. J. (2009). Two sides of the same coin no longer: genetic separation of nociceptive sensitization responses. *Commun. Integr. Biol.* **2**, 517-519.

Babcock, D. T., Landry, C. and Galko, M. J. (2009). Cytokine signaling mediates UV-induced nociceptive sensitization in *Drosophila* larvae. *Curr. Biol.* **19**, 799-806.

Babcock, D. T., Shi, S., Jo, J., Shaw, M., Gutstein, H. B. and Galko, M. J. (2011). Hedgehog signaling regulates nociceptive sensitization. *Curr. Biol.* **21**, 1525-1533.

Bellen, H. J., Tong, C. and Tsuda, H. (2010). 100 years of *Drosophila* research and its impact on vertebrate neuroscience: a history lesson for the future. *Nat. Rev. Neurosci.* **11**, 514-522.

Bierhaus, A., Fleming, T., Stoyanov, S., Leffler, A., Babes, A., Neacsu, C., Sauer, S. K., Eberhardt, M., Schnölzer, M., Lasitschka, F. et al. (2012). Methylglyoxal modification of Nav1.8 facilitates nociceptive neuron firing and causes hyperalgesia in diabetic neuropathy. *Nat. Med.* **18**, 926-933.

Bruning, J. C., Gautam, D., Burks, D. J., Gillette, J., Schubert, M., Orban, P. C., Klein, R., Krone, W., Muller-Wieland, D. and Kahn, C. R. (2000). Role of brain insulin receptor in control of body weight and reproduction. *Science* **289**, 2122-2125.

Brussee, V., Cunningham, F. A. and Zochodne, D. W. (2004). Direct insulin signaling of neurons reverses diabetic neuropathy. *Diabetes* **53**, 1824-1830.

Chan, A. W., Macfarlane, I. A. and Bowsher, D. (1990). Short term fluctuations in blood glucose concentrations do not alter pain perception in diabetic-patients with and without painful peripheral neuropathy. *Diabetes Res.* **14**, 15-19.

Chattopadhyay, A., Gilstrap, A. V. and Galko, M. J. (2012). Local and global methods of assessing thermal nociception in *Drosophila* larvae. *J. Vis. Exp.* e3837.

Chen, C., Jack, J. and Garofalo, R. S. (1996). The *Drosophila* insulin receptor is required for normal growth. *Endocrinology* **137**, 846-856.

Chen, T.-W., Wardill, T. J., Sun, Y., Pulver, S. R., Renninger, S. L., Baohan, A., Schreiter, E. R., Kerr, R. A., Orger, M. B., Jayaraman, V. et al. (2013). Ultrasensitive fluorescent proteins for imaging neuronal activity. *Nature* **499**, 295-300.

Chiu, S.-L., Chen, C.-M. and Cline, H. T. (2008). Insulin receptor signaling regulates synapse number, dendritic plasticity, and circuit function in vivo. *Neuron* **58**, 708-719.

Das, R., Bhattacharjee, S., Patel, A. A., Harris, J. M., Bhattacharya, S., Letcher, J. M., Clark, S. G., Nanda, S., Iyer, E. P. R., Ascoli, G. A. et al. (2017). Dendritic cytoskeletal architecture is modulated by combinatorial transcriptional regulation in *Drosophila melanogaster*. *Genetics* **207**, 1401-1421.

Demontis, F. and Perrimon, N. (2010). FOXO/4E-BP signaling in *Drosophila* muscles regulates organism-wide proteostasis during aging. *Cell* **143**, 813-825.

Dietzl, G., Chen, D., Schnorrer, F., Su, K.-C., Barinova, Y., Fellner, M., Gasser, B., Kinsey, K., Oettel, S., Scheiblaue, S. et al. (2007). A genome-wide transgenic RNAi library for conditional gene inactivation in *Drosophila*. *Nature* **448**, 151-156.

Enjin, A., Zaharieva, E. E., Frank, D. D., Mansourian, S., Suh, G. S. B., Gallio, M. and Stensmyr, M. C. (2016). Humidity sensing in *Drosophila*. *Curr. Biol.* **26**, 1352-1358.

Fernandez, R., Tabarini, D., Azpiaz, N., Frasc, M. and Schlessinger, J. (1995). The *Drosophila* insulin receptor homolog: a gene essential for embryonic development encodes two receptor isoforms with different signaling potential. *EMBO J.* **14**, 3373-3384.

Fernyhough, P., Willars, G. B., Lindsay, R. M. and Tomlinson, D. R. (1993). Insulin and insulin-like growth factor I enhance regeneration in cultured adult rat sensory neurones. *Brain Res.* **607**, 117-124.

Fosque, B. F., Sun, Y., Dana, H., Yang, C. T., Ohyama, T., Tadross, M. R., Patel, R., Zlatich, M., Kim, D. S., Ahrens, M. B. et al. (2015). Neural circuits. Labeling of active neural circuits in vivo with designed calcium integrators. *Science* **347**, 755-760.

Gao, F.-B., Brenman, J. E., Jan, L. Y. and Jan, Y. N. (1999). Genes regulating dendritic outgrowth, branching, and routing in *Drosophila*. *Genes Dev.* **13**, 2549-2561.

Gold, M. S. and Gebhart, G. F. (2010). Nociceptor sensitization in pain pathogenesis. *Nat. Med.* **16**, 1248-1257.

Graham, P. and Pick, L. (2017). *Drosophila* as a model for diabetes and diseases of insulin resistance. *Curr. Top. Dev. Biol.* **121**, 397-419.

Gralle, M. (2017). The neuronal insulin receptor in its environment. *J. Neurochem.* **140**, 359-367.

Grillo, C. A., Piroli, G. G., Lawrence, R. C., Wrihten, S. A., Green, A. J., Wilson, S. P., Sakai, R. R., Kelly, S. J., Wilson, M. A., Mott, D. D. et al. (2015). Hippocampal insulin resistance impairs spatial learning and synaptic plasticity. *Diabetes* **64**, 3927-3936.

Grote, C. W. and Wright, D. E. (2016). A role for insulin in diabetic neuropathy. *Front. Neurosci.* **10**, 581.

Grote, C. W., Groover, A. L., Ryals, J. M., Geiger, P. C., Feldman, E. L. and Wright, D. E. (2013). Peripheral nervous system insulin resistance in ob/ob mice. *Acta Neuropathol. Commun.* **1**, 15.

- Grueter, W. B., Jan, L. Y. and Jan, Y. N. (2002). Tiling of the Drosophila epidermis by multidendritic sensory neurons. *Development* **129**, 2867-2878.
- Himmel, N. J., Patel, A. A. and Cox, D. N. (2017). Invertebrate Nociception. In *Oxford Research Encyclopedia of Neuroscience*. New York: Oxford University Press.
- Hu, C., Petersen, M., Hoyer, N., Spitzweck, B., Tenedini, F., Wang, D., Gruschka, A., Burchardt, L. S., Szpotowicz, E., Schweizer, M. et al. (2017). Sensory integration and neuromodulatory feedback facilitate Drosophila mechanonociceptive behavior. *Nat. Neurosci.* **20**, 1085-1095.
- Hwang, R. Y., Zhong, L., Xu, Y., Johnson, T., Zhang, F., Deisseroth, K. and Tracey, W. D. (2007). Nociceptive neurons protect Drosophila larvae from parasitoid wasps. *Curr. Biol.* **17**, 2105-2116.
- Ikeya, T., Galic, M., Belawat, N., Nairz, K. and Hafen, E. (2002). Nutrient-dependent expression of insulin-like peptides from neuroendocrine cells in the CNS contributes to growth regulation in Drosophila. *Curr. Biol.* **12**, 1293-1300.
- Im, S. H. and Galko, M. J. (2012). Pokes, sunburn, and hot sauce: Drosophila as an emerging model for the biology of nociception. *Dev. Dyn.* **241**, 16-26.
- Im, S. H., Takle, K., Jo, J., Babcock, D. T., Ma, Z., Xiang, Y. and Galko, M. J. (2015). Tachykinin acts upstream of autocrine Hedgehog signaling during nociceptive sensitization in Drosophila. *eLife* **4**, e10735.
- Iyer, E. P. R., Iyer, S. C., Sullivan, L., Wang, D., Meduri, R., Graybeal, L. L. and Cox, D. N. (2013). Functional genomic analyses of two morphologically distinct classes of Drosophila sensory neurons: post-mitotic roles of transcription factors in dendritic patterning. *PLoS ONE* **8**, e72434.
- Karpac, J., Younger, A. and Jasper, H. (2011). Dynamic coordination of innate immune signaling and insulin signaling regulates systemic responses to localized DNA damage. *Dev Cell* **20**, 841-854.
- Kennedy, W. R., Wendelschafer-Crabb, G. and Johnson, T. (1996). Quantitation of epidermal nerves in diabetic neuropathy. *Neurology* **47**, 1042-1048.
- Kim, S. K. and Rulifson, E. J. (2004). Conserved mechanisms of glucose sensing and regulation by Drosophila corpora cardiaca cells. *Nature* **431**, 316-320.
- Kim, B., Mclean, L. L., Philip, S. S. and Feldman, E. L. (2011). Hyperinsulinemia induces insulin resistance in dorsal root ganglion neurons. *Endocrinology* **152**, 3638-3647.
- Lilja, J., Laulund, F. and Forsby, A. (2007). Insulin and insulin-like growth factor type-1 up-regulate the vanilloid receptor-1 (TRPV1) in stably TRPV1-expressing SH-SY5Y neuroblastoma cells. *J. Neurosci.* **27**, 1413-1419.
- Martin-Pena, A., Acebes, A., Rodriguez, J.-R., Sorribes, A., de Polavieja, G. G., Fernandez-Funez, P. and Ferrus, A. (2006). Age-independent synaptogenesis by phosphoinositide 3 kinase. *J. Neurosci.* **26**, 10199-10208.
- Morris, S. N. S., Coogan, C., Chamseddin, K., Fernandez-Kim, S. O., Kolli, S., Keller, J. N. and Bauer, J. H. (2012). Development of diet-induced insulin resistance in adult Drosophila melanogaster. *Biochim. Biophys. Acta* **1822**, 1230-1237.
- Musselman, L. P., Fink, J. L., Narzinski, K., Ramachandran, P. V., Hathiramani, S. S., Cagan, R. L. and Baranski, T. J. (2011). A high-sugar diet produces obesity and insulin resistance in wild-type Drosophila. *Dis. Model. Mech.* **4**, 842-849.
- Musselman, L. P., Fink, J. L., Grant, A. R., Gatto, J. A., Tuthill, B. F., II and Baranski, T. J. (2017). The relationship between immunity and metabolism in Drosophila diet-induced insulin resistance. *Mol. Cell. Biol.* **38**, e00259-17.
- Na, J., Musselman, L. P., Pendse, J., Baranski, T. J., Bodmer, R., Ocorr, K. and Cagan, R. (2013). A Drosophila model of high sugar diet-induced cardiomyopathy. *PLoS Genet.* **9**, e1003175.
- Ni, J.-Q., Zhou, R., Czech, B., Liu, L.-P., Holderbaum, L., Yang-Zhou, D., Shim, H.-S., Tao, R., Handler, D., Karpowicz, P. et al. (2011). A genome-scale shRNA resource for transgenic RNAi in Drosophila. *Nat. Methods* **8**, 405-407.
- Obrosova, I. G. (2009). Diabetic painful and insensate neuropathy: pathogenesis and potential treatments. *Neurotherapeutics* **6**, 638-647.
- Ohyama, T., Schneider-Mizell, C. M., Fetter, R. D., Aleman, J. V., Franconville, R., Rivera-Alba, M., Mensh, B. D., Branson, K. M., Simpson, J. H., Truman, J. W., Cardona, A. and Zlatic, M. (2015). A multilevel multimodal circuit enhances action selection in Drosophila. *Nature* **520**, 633-639.
- Orestes, P., Osuru, H. P., Mcintire, W. E., Jacus, M. O., Salajegheh, R., Jagodic, M. M., Choe, W., Lee, J., Lee, S.-S., Rose, K. E. et al. (2013). Reversal of neuropathic pain in diabetes by targeting glycosylation of Ca(V)3.2 T-type calcium channels. *Diabetes* **62**, 3828-3838.
- Park, S., Alfa, R. W., Topper, S. M., Kim, G. E. S., Kockel, L. and Kim, S. K. (2014). A genetic strategy to measure circulating Drosophila insulin reveals genes regulating insulin production and secretion. *PLoS Genet.* **10**, e1004555.
- Patel, A. A. and Cox, D. N. (2017). Behavioral and functional assays for investigating mechanisms of noxious cold detection and multimodal sensory processing in Drosophila larvae. *Biol. Protoc.* **7**, e2388.
- Powell, H. C., Rosoff, J. and Myers, R. R. (1985). Microangiopathy in human diabetic neuropathy. *Acta Neuropathol.* **68**, 295-305.
- Recio-Pinto, E., Rechler, M. M. and Ishii, D. N. (1986). Effects of insulin, insulin-like growth factor-I, and nerve growth factor on neurite formation and survival in cultured sympathetic and sensory neurons. *J. Neurosci.* **6**, 1211-1219.
- Rodenfels, J., Lavrynenko, O., Ayciriex, S., Sampaio, J. L., Carvalho, M., Shevchenko, A. and Eaton, S. (2014). Production of systemically circulating Hedgehog by the intestine couples nutrition to growth and development. *Genes Dev.* **28**, 2636-2651.
- Romanovsky, D., Wang, J., Al-Chaer, E. D., Stimers, J. R. and Dobretsov, M. (2010). Comparison of metabolic and neuropathy profiles of rats with streptozotocin-induced overt and moderate insulinopenia. *Neuroscience* **170**, 337-347.
- Rulifson, E. J., Kim, S. K. and Nusse, R. (2002). Ablation of insulin-producing neurons in flies: growth and diabetic phenotypes. *Science* **296**, 1118-1120.
- Sinenko, S. A. and Mathey-Prevot, B. (2004). Increased expression of Drosophila tetraspanin, Tsp68c, suppresses the abnormal proliferation of ytr-deficient and Ras/Raf-activated hemocytes. *Oncogene* **23**, 9120-9128.
- Skorupa, D. A., Dervisevendic, A., Zwiener, J. and Pletcher, S. D. (2008). Dietary composition specifies consumption, obesity, and lifespan in Drosophila melanogaster. *Aging Cell* **7**, 478-490.
- Song, W., Onishi, M., Jan, L. Y. and Jan, Y. N. (2007). Peripheral multidendritic sensory neurons are necessary for rhythmic locomotion behavior in Drosophila larvae. *Proc. Natl. Acad. Sci. USA* **104**, 5199-5204.
- Sugimoto, K., Murakawa, Y., Zhang, W., Xu, G. and Sima, A. A. F. (2000). Insulin receptor in rat peripheral nerve: its localization and alternatively spliced isoforms. *Diabetes Metab. Res. Rev.* **16**, 354-363.
- Sugimoto, K., Murakawa, Y. and Sima, A. A. F. (2002). Expression and localization of insulin receptor in rat dorsal root ganglion and spinal cord. *J. Peripher. Nerv. Syst.* **7**, 44-53.
- Tatar, M., Kopelman, A., Epstein, D., Tu, M. P., Yin, C. M. and Garofalo, R. S. (2001). A mutant Drosophila insulin receptor homolog that extends life-span and impairs neuroendocrine function. *Science* **292**, 107-110.
- Teleman, A. A. (2010). Molecular mechanisms of metabolic regulation by insulin in Drosophila. *Biochem. J.* **425**, 13-26.
- Tsantoulas, C., Láinez, S., Wong, S., Mehta, I., Vilar, B. and Mcnaughton, P. A. (2017). Hyperpolarization-activated cyclic nucleotide-gated 2 (HCN2) ion channels drive pain in mouse models of diabetic neuropathy. *Sci. Transl. Med.* **9**, eaam6072.
- Turner, H. N., Armengol, K., Patel, A. A., Himmel, N. J., Sullivan, L., Iyer, S. C., Bhattacharya, S., Iyer, E. P. R., Landry, C., Galko, M. J. et al. (2016). The TRP channels Pkd2, Nompcc, and Trpm act in cold-sensing neurons to mediate unique aversive behaviors to noxious cold in Drosophila. *Curr. Biol.* **26**, 3116-3128.
- Veves, A., Backonja, M. and Malik, R. A. (2008). Painful diabetic neuropathy: epidemiology, natural history, early diagnosis, and treatment options. *Pain Med.* **9**, 660-674.
- Wang, Y., Wang, L. and Wang, Z. (2008). Transgenic analyses of TGIF family proteins in Drosophila imply their role in cell growth. *J. Genet. Genomics* **35**, 457-465.
- Wang, H., Heijnen, C. J., Eijkelkamp, N., Carbajal, A. G., Schedlowski, M., Kelley, K. W., Dantzer, R. and Kavelaars, A. (2011). GRK2 in sensory neurons regulates epinephrine-induced signalling and duration of mechanical hyperalgesia. *Pain* **152**, 1649-1658.
- Wessells, R. J., Fitzgerald, E., Cypser, J. R., Tatar, M. and Bodmer, R. (2004). Insulin regulation of heart function in aging fruit flies. *Nat. Genet.* **36**, 1275-1281.
- Wright, D. E., Johnson, M. S., Arnett, M. G., Smittkamp, S. E. and Ryals, J. M. (2007). Selective changes in nocifensive behavior despite normal cutaneous axon innervation in leptin receptor-null mutant (db/db) mice. *J. Peripher. Nerv. Syst.* **12**, 250-261.
- Wu, Q., Zhang, Y., Xu, J. and Shen, P. (2005). Regulation of hunger-driven behaviors by neural ribosomal S6 kinase in Drosophila. *Proc. Natl. Acad. Sci. USA* **102**, 13289-13294.
- Wu, Y., Brock, A. R., Wang, Y., Fujitani, K., Ueda, R. and Galko, M. J. (2009). A blood-borne PDGF/VEGF-like ligand initiates wound-induced epidermal cell migration in Drosophila larvae. *Curr. Biol.* **19**, 1473-1477.
- Yoshino, J., Morikawa, R. K., Hasegawa, E. and Emoto, K. (2017). Neural circuitry that evokes escape behavior upon activation of nociceptive sensory neurons in Drosophila larvae. *Curr. Biol.* **27**, 2499-2504.e3.
- Zars, T., Fischer, M., Schulz, R. and Heisenberg, M. (2000). Localization of a short-term memory in Drosophila. *Science* **288**, 672-675.
- Zochodne, D. W. (2016). Sensory neurodegeneration in diabetes: beyond glucotoxicity. *Int. Rev. Neurobiol.* **127**, 151-180.
- Zolnik, T. A., Sha, F., Johnenning, F. W., Schreiter, E. R., Looger, L. L., Larkum, M. E. and Sachdev, R. N. S. (2017). All-optical functional synaptic connectivity mapping in acute brain slices using the calcium integrator CaMPARI. *J. Physiol.* **595**, 1465-1477.

Supplementary Table 1: Gal4 Driver lines used.

Gal4	Tissues	References
<i>Gal4</i> ¹⁰⁹⁽²⁾⁸⁰ (<i>md-Gal4</i>)	multi-dendritic sensory neurons	(Gao et al., 1999)
<i>21-7-Gal4</i>	multi-dendritic sensory neurons	(Song et al., 2007)
<i>ppk1.9-Gal4</i>	class IV nociceptive md sensory neurons	(Ainsley et al., 2003)
<i>dilp2-Gal4</i>	Insulin Producing Cells	(Rulifson et al., 2002)
<i>hmlΔ-Gal4</i>	hemocytes	(Sinenko and Mathey-Prevot, 2004)
<i>Dmef2-Gal4</i>	larval muscles	(Zars et al., 2000)
<i>Gal4</i> ^{OK376} (<i>FB-Gal4</i>)	larval fat body	(Wu et al., 2009)

Supplementary Table 2: Genotypes of larvae used in this study

Figure 1	<i>w</i> ¹¹¹⁸ <i>w</i> ¹¹¹⁸ ; ; <i>InR</i> ^{e19} /+ <i>w</i> ¹¹¹⁸ ; ; <i>InR</i> ^{93Dj4} /+ <i>w</i> ¹¹¹⁸ ; ; <i>InR</i> ^{e19/93Dj4}
Figure 2B-2D	<i>w</i> ¹¹¹⁸ ; <i>dilp2-Gal4</i> / <i>ppkCD4tdTOM</i> <i>w</i> ¹¹¹⁸ ; <i>ppkCD4tdTOM</i> /+; <i>UAS-Kir2.1</i> /+ <i>w</i> ¹¹¹⁸ ; <i>dilp2-Gal4/ppkCD4tdTOM</i> ; <i>UAS-Kir2.1</i> /+
Figure 2E-2F	<i>w</i> ¹¹¹⁸ ; <i>dilp2-Gal4</i> /+ <i>w</i> ¹¹¹⁸ ; ; <i>UAS-Kir2.1</i> /+ <i>w</i> ¹¹¹⁸ ; <i>dilp2-Gal4</i> /+; <i>UAS-Kir2.1</i> /+
Figure 3B-3D	<i>w</i> ¹¹¹⁸ ; <i>ppkCD4tdTOM</i>
Figure 3E-3H	<i>w</i> ¹¹¹⁸
Figure 4A-4D	<i>w</i> ¹¹¹⁸ ; <i>Gal4</i> ¹⁰⁹⁽²⁾⁸⁰ /+ <i>w</i> ¹¹¹⁸ ; ; <i>UAS-InR</i> ^{RNAi(JF01482)} /+ <i>w</i> ¹¹¹⁸ ; ; <i>UAS-InR</i> ^{RNAi(JF01183)} /+ <i>w</i> ¹¹¹⁸ ; <i>Gal4</i> ¹⁰⁹⁽²⁾⁸⁰ /+; <i>UAS-InR</i> ^{RNAi(JF01482)} /+ <i>w</i> ¹¹¹⁸ ; <i>Gal4</i> ¹⁰⁹⁽²⁾⁸⁰ /+; <i>UAS-InR</i> ^{RNAi(JF01183)} /+
Figure 4E-4G	<i>w</i> ¹¹¹⁸ ; ; <i>UAS-InR</i> ^{RNAi(JF01482)} / <i>ppk1.9-Gal4</i> , <i>UAS-mCD8::GFP</i> <i>w</i> ¹¹¹⁸ ; ; <i>UAS-Luc</i> ^{RNAi} / <i>ppk1.9-Gal4</i> , <i>UAS-mCD8::GFP</i>
Figure 5	<i>w</i> ¹¹¹⁸ ; <i>Gal4</i> ¹⁰⁹⁽²⁾⁸⁰ / <i>UAS-CaMPARI</i> ; <i>UAS-InR</i> ^{RNAi(JF01482)} /+

$w^{1118}; Gal4^{109(2)80}/UAS-CaMPARI$

Figure 6

$w^{1118}; Gal4^{109(2)80}/+$
 $w^{1118}; UAS-InR^{CA(A1325D)}/+$
 $w^{1118}; Gal4^{109(2)80}/+; UAS-InR^{CA(A1325D)}/+$

Figure 7A-7C

$w^{1118}; Gal4^{109(2)80}/+; InR^{e19}/+$
 $w^{1118}; UAS-InR/+; InrR^{e19}/+$
 $w^{1118}; Gal4^{109(2)80}/UAS-InR; InR^{e19}/+$

Figure 7D-7F

$w^{1118}; Gal4^{109(2)80}/+;$
 $w^{1118}; UAS-InR^{CA(A1325D)}/+$
 $w^{1118}; Gal4^{109(2)80}/+; UAS-InR^{CA(A1325D)}/+$

Figure S1

w^{1118}
 $w^{1118}; InR^{e19}/+$
 $w^{1118}; InR^{93Dj4}/+$
 $w^{1118}; InR^{e19/93Dj4}$

Figure S2

$w^{1118}; Gal4^{OK376}/+$
 $w^{1118}; Gal4^{OK376}/+; UAS-InR^{RNAi(JF01482)}/+$
 $w^{1118}; Dmef2-Gal4/+$
 $w^{1118}; Dmef2-Gal4/UAS-InR^{RNAi(JF01482)}$
 $w^{1118}; hml\Delta-Gal4, UAS-GFP/+$
 $w^{1118}; hml\Delta-Gal4, UAS-GFP/+; UAS-InR^{RNAi(JF01482)}/+$

Figure S3

$w^{1118}; 21-7-Gal4/+$
 $w^{1118}; 21-7-Gal4/+; UAS-InR^{RNAi(JF01482)}/+$

Figure S4

$w^{1118}; ppk1.9-Gal4/+$
 $w^{1118}; ppk1.9-Gal4/UAS-InR^{RNAi(JF01482)}$

Figure S6

$w^{1118}; Gal4^{109(2)80}/+$
 $w^{1118}; UAS-InR^{DN(1)}/+$
 $w^{1118}; UAS-InR^{DN(2)}/+$
 $w^{1118}; Gal4^{109(2)80}/UAS-InR^{DN(1)}/+$
 $w^{1118}; Gal4^{109(2)80}/+; UAS-InR^{DN(2)}/+$

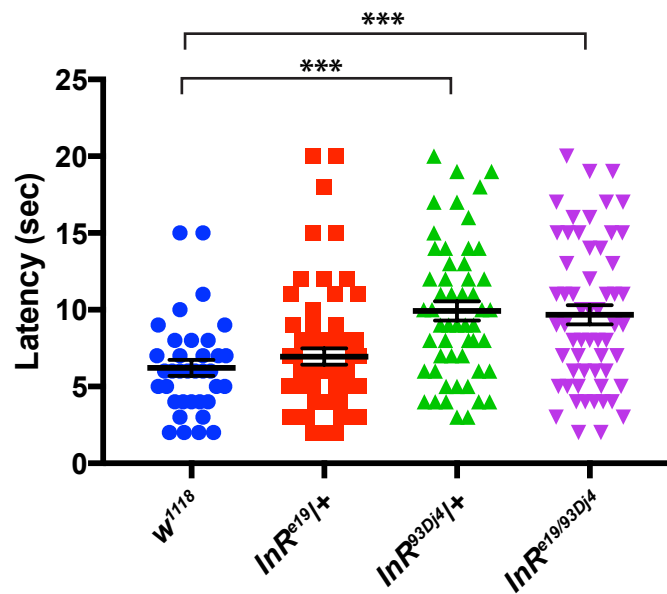
Figure S7

$w^{1118}; Gal4^{109(2)80}/+$
 $w^{1118}; Gal4^{109(2)80}/+; UAS-chico^{RNAi(JF02964)}/+$
 $w^{1118}; Gal4^{109(2)80}/+; UAS-Pi3K68D^{RNAi(GD7348)}/+$
 $w^{1118}; Gal4^{109(2)80}/+; UAS-Pi3K92E^{RNAi(GD11228)}/+$

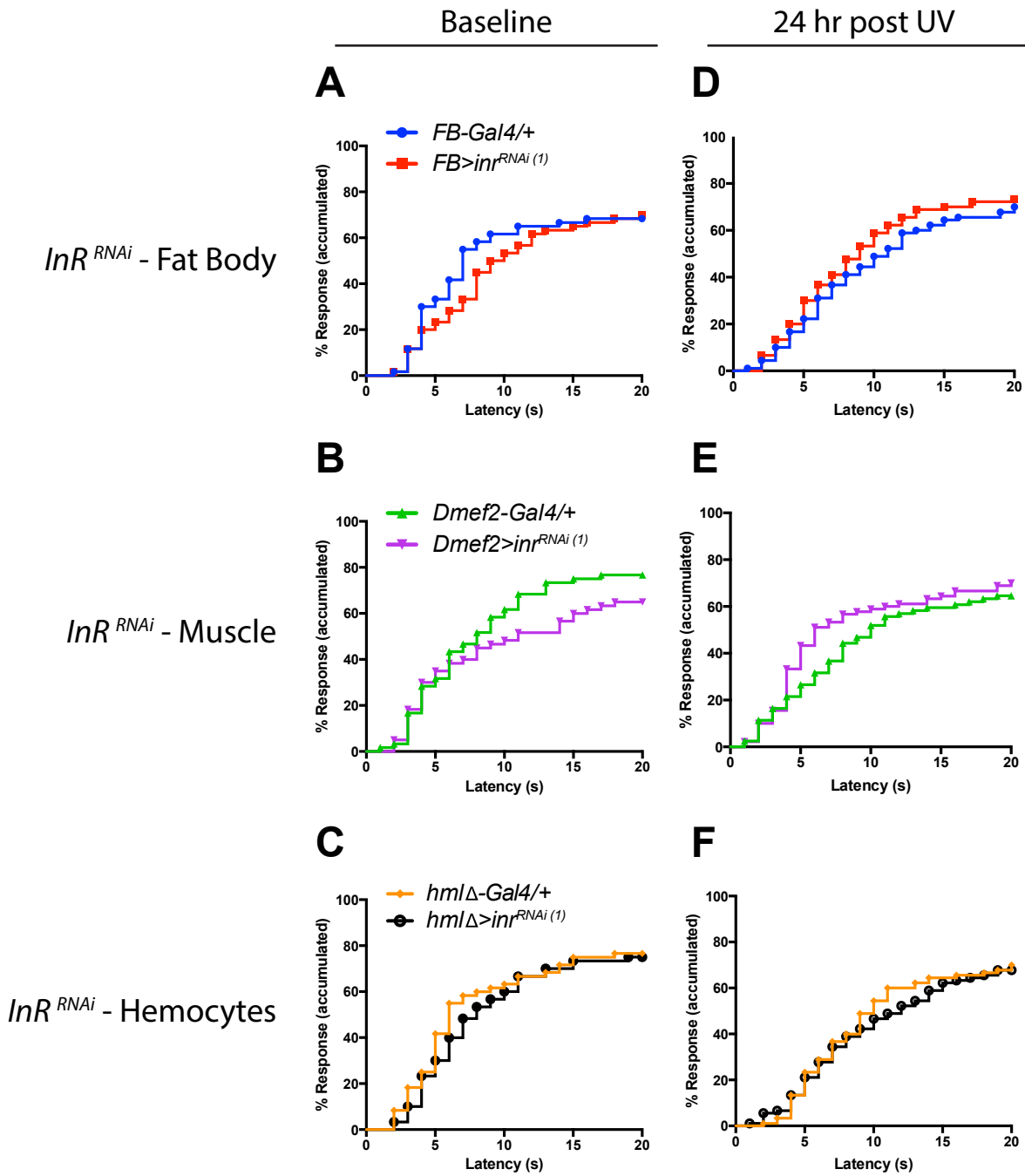
References

- AINSLEY, J. A., PETTUS, J. M., BOSENKO, D., GERSTEIN, C. E., ZINKEVICH, N., ANDERSON, M. G., ADAMS, C. M., WELSH, M. J. & JOHNSON, W. A. 2003. Enhanced locomotion caused by loss of the Drosophila DEG/ENaC protein Pickpocket1. *Curr Biol*, 13, 1557-63.
- GAO, F. B., BRENMAN, J. E., JAN, L. Y. & JAN, Y. N. 1999. Genes regulating dendritic outgrowth, branching, and routing in Drosophila. *Genes Dev*, 13, 2549-61.
- RULIFSON, E. J., KIM, S. K. & NUSSE, R. 2002. Ablation of insulin-producing neurons in flies: growth and diabetic phenotypes. *Science*, 296, 1118-20.
- SINENKO, S. A. & MATHEY-PREVOT, B. 2004. Increased expression of Drosophila tetraspanin, Tsp68C, suppresses the abnormal proliferation of ytr-deficient and Ras/Raf-activated hemocytes. *Oncogene*, 23, 9120-8.
- SONG, W., ONISHI, M., JAN, L. Y. & JAN, Y. N. 2007. Peripheral multidendritic sensory neurons are necessary for rhythmic locomotion behavior in Drosophila larvae. *Proc Natl Acad Sci U S A*, 104, 5199-204.
- WU, Y., BROCK, A. R., WANG, Y., FUJITANI, K., UEDA, R. & GALKO, M. J. 2009. A blood-borne PDGF/VEGF-like ligand initiates wound-induced epidermal cell migration in Drosophila larvae. *Curr Biol*, 19, 1473-7.
- ZARS, T., FISCHER, M., SCHULZ, R. & HEISENBERG, M. 2000. Localization of a short-term memory in Drosophila. *Science*, 288, 672-5.

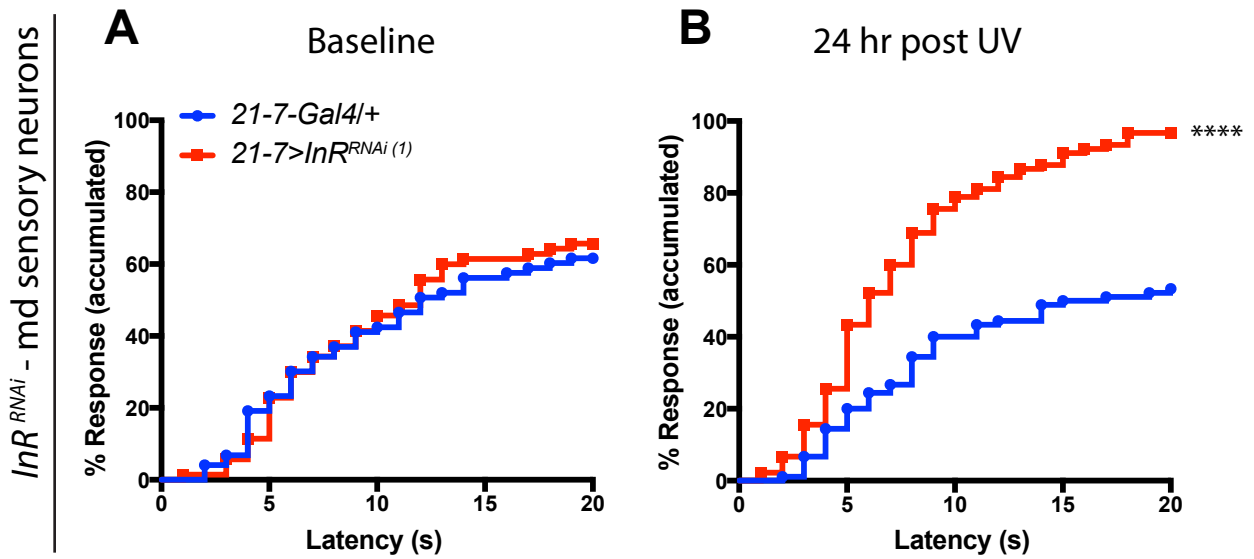
Supplementary Figures



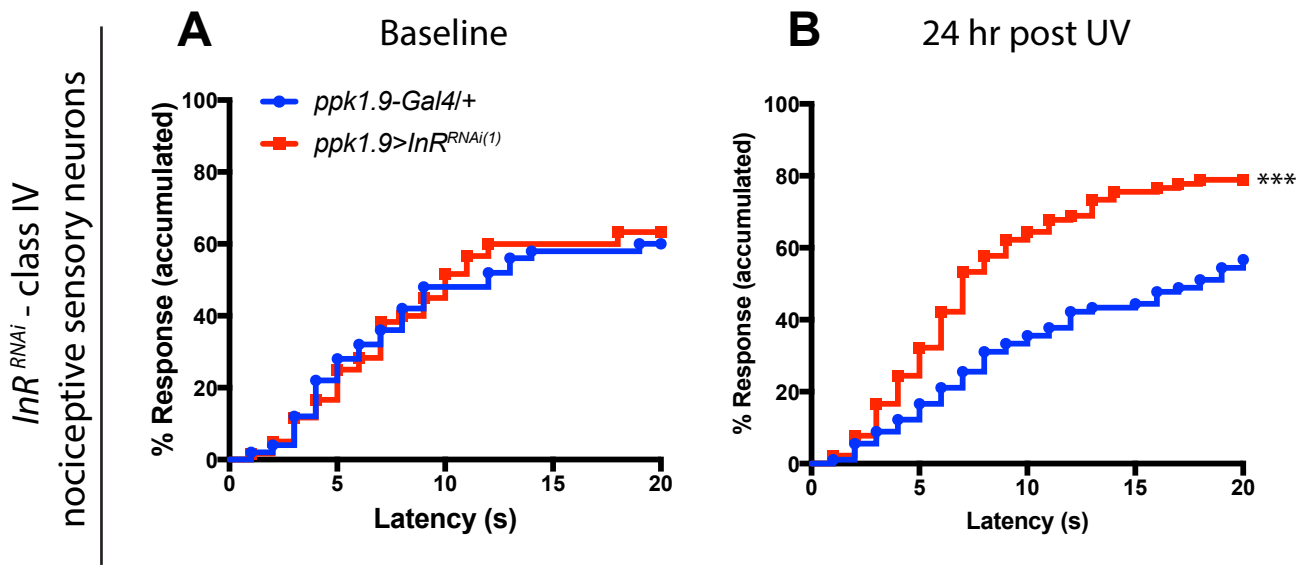
Supplementary Figure 1. InR mutant larvae show a mild increase in latency of thermal nociceptive behavior in the absence of UV injury. The data from Figure 1C (baseline, 43 °C thermal stimuli) are plotted to compare the average latency of each group. Each data point = an observed latency; middle bar = mean; error bar = standard deviation. Statistics: one-way ANOVA with Dunnett's multiple comparison post-hoc test.



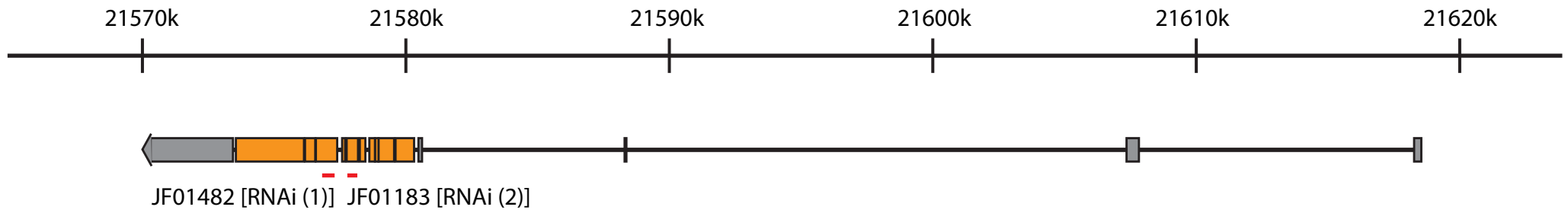
Supplementary Figure 2. Knock down of Insulin Receptor in other tissues does not cause persistent thermal hyperalgesia. Quantitation of nociceptive behavioral responses to thermal stimulation at 43 °C when *UAS-InR^{RNAi}* is expressed in the indicated tissues. (A-C) Baseline responses without UV-induced tissue damage (n = 90). (A) Fat body, (B) Muscle, (C) Hemocytes. (D-F) Thermal sensitivity at 24 hours post UV. (D) Fat body (n = 90), (E) Muscle (n = 79 for *Dmef2-Gal4* alone control, 90 for RNAi), (F) Hemocytes (n = 90). See Table S1 for Gal4 Driver specifics.



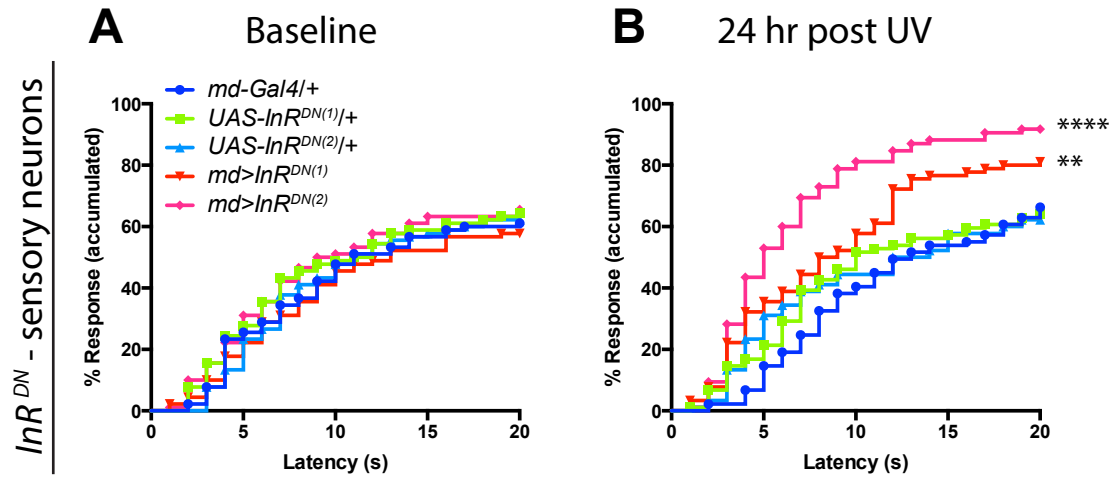
Supplementary Figure 3. Expression of $UAS-InR^{RNAi}$ via an alternative md neuron-specific Gal4 driver also causes persistent thermal hyperalgesia. Quantitation of nociceptive behavioral responses to thermal stimulation at 43 °C when $UAS-InR^{RNAi}$ is expressed via the md sensory neuron-specific driver *21-7-Gal4*. (A) Baseline responses without UV-induced tissue damage (n = 73 for *21-7-Gal4* alone control, 70 for RNAi). (B) Thermal sensitivity at 24 hours post UV. (n = 90).



Supplementary Figure 4. Expression of *UAS-InR^{RNAi}* via a class IV md neuron-specific Gal4 driver also causes persistent thermal hyperalgesia. Quantitation of nociceptive behavioral responses to thermal stimulation at 43 °C when *UAS-InR^{RNAi}* is expressed via class IV nociceptive neuron-specific driver (*ppk1.9-Gal4*). (A) Baseline responses without UV-induced tissue damage (n = 50 for *ppk1.9-Gal4* alone control, 60 for RNAi). (B) Thermal sensitivity at 24 hours post UV. (n = 90).



Supplementary Figure 5. Schematic of the *InR* locus and position of *UAS-RNAi* transgenes targeting *InR*. Two of non-overlapping RNAi lines targeting *InR* were used. JF01482 = *UAS-InR^{RNAi (1)}*; JF01183 = *UAS-InR^{RNAi (2)}*.



Supplementary Figure 6. Sensory neuron-specific expression of a dominant negative form

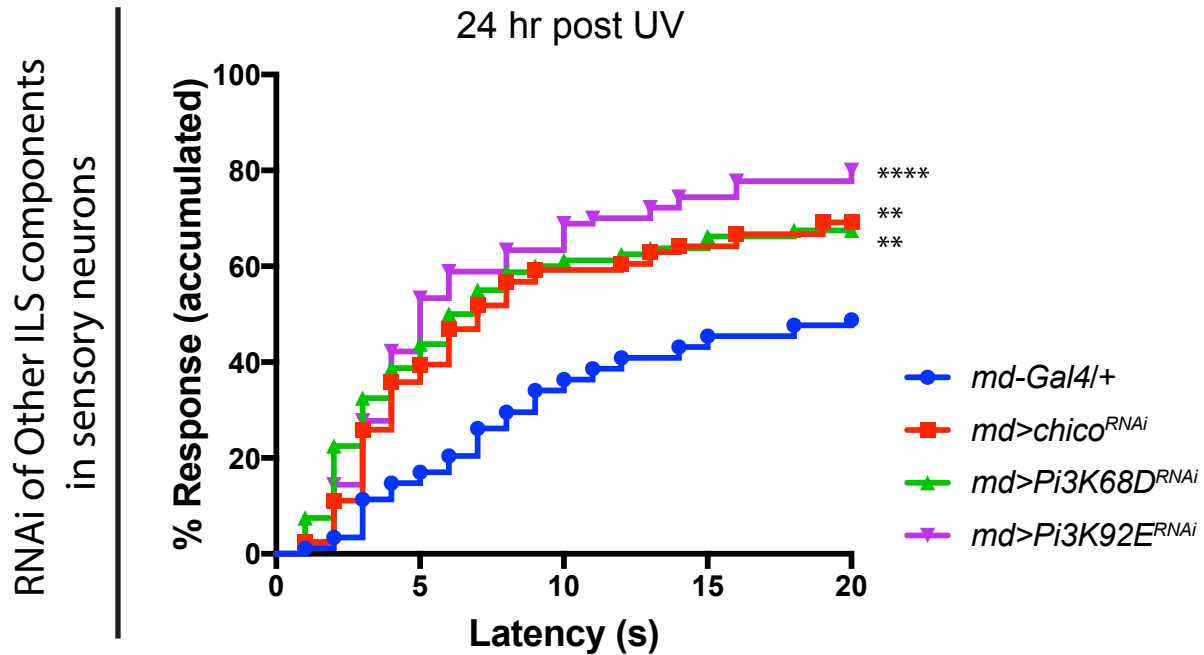
of the Insulin Receptor causes persistent thermal hyperalgesia. Quantitation of nociceptive

behavioral responses to thermal stimulation at 43 °C when *UAS-InR^{DN}* is expressed in *md*

sensory neurons. (A) Baseline responses without UV-induced tissue damage (n = 90). (B)

Thermal sensitivity at 24 hours post UV (n = 89 for *md-Gal4*, *UAS-InR^{DN(1)}*, 85 for *md> InR^{DN(2)}*,

90 for the rest).



Supplementary Figure 7. *md* neuron-specific expression of RNAi transgenes targeting other components of ILS also causes persistent thermal hyperalgesia. Quantitation of nociceptive behavioral responses to thermal stimulation at 43 °C when *UAS-RNAi* transgenes targeting signaling components of the ILS pathway are expressed in *md* sensory neurons. Thermal sensitivity at 24 hours post UV (n = 88 for *md-Gal4* alone control, 81 for *chico^{RNAi}*, 80 for *Pi3K68D^{RNAi}*, 90 for *Pi3K92E^{RNAi}*).